

Controlling Amyloid Beta Peptide Aggregation and Toxicity by Protease-Stable Ligands

Rathnam Mallesh, Juhee Khan, Prabir Kumar Gharai, Varsha Gupta, Rajsekhar Roy, and Surajit Ghosh*

Cite This: *ACS Bio Med Chem Au* 2023, 3, 158–173

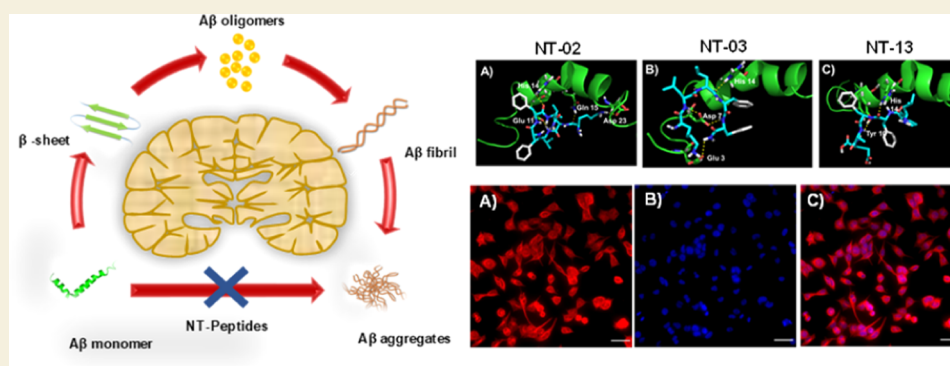
Read Online

ACCESS |

Metrics & More

Article Recommendations

Supporting Information



ABSTRACT: Polymerization of soluble amyloid beta ($A\beta$) peptide into protease-stable insoluble fibrillary aggregates is a critical step in the pathogenesis of Alzheimer's disease (AD). The N-terminal (NT) hydrophobic central domain fragment 16KLVFF20 plays an important role in the formation and stabilization of β -sheets by self-recognition of the parent $A\beta$ peptide, followed by aggregation of $A\beta$ in the AD brain. Here, we analyze the effect of the NT region inducing β -sheet formation in the $A\beta$ peptide by a single amino acid mutation in the native $A\beta$ peptide fragment. We designed 14 hydrophobic peptides (NT-01 to NT-14) by a single mutation at 18Val by using hydrophobic residues leucine and proline in the natural $A\beta$ peptide fragment (KLVFFAE) and analyzed its effect on the formation of $A\beta$ aggregates. Among all these peptides, NT-02, NT-03, and NT-13 significantly affected the $A\beta$ aggregate formation. When the NT peptides were coincubated with the $A\beta$ peptide, a significant reduction in β -sheet formation and increment in random coil content of $A\beta$ was seen, confirmed by circular dichroism spectroscopy and Fourier transform infrared spectroscopy, followed by the reduction of fibril formation measured by the thioflavin-T (ThT) binding assay. The aggregation inhibition was monitored by Congo red and ThT staining and electron microscopic examination. Moreover, the NT peptides protect the PC-12 differentiated neurons from $A\beta$ -induced toxicity and apoptosis in vitro. Thus, manipulation of the $A\beta$ secondary structure with protease-stable ligands that promote the random coil conformation may provide a tool to control the $A\beta$ aggregates observed in AD patients.

KEYWORDS: amyloid beta, Alzheimer's disease, β -sheet breakers, neuroprotection, protease-stable ligands

INTRODUCTION

The amyloid beta ($A\beta$) peptide is the most important protein constituent in neuritic senile plaques¹ and cerebrovascular amyloid deposition.^{2,3} Overproduction and polymerization of the $A\beta$ peptide into protease-stable insoluble aggregates is a major step in the pathogenesis of Alzheimer's disease (AD).⁴ In physiological conditions, the $A\beta$ peptide easily aggregates into fibrillary β -sheets and then it forms insoluble aggregates.⁵ In the provision of this argument, particular mutations in the gene encoding the amyloid beta-precursor protein (APP),⁶ which leads to excess production of $A\beta$ peptide with heterogenic structural variants ($A\beta$ 40, $A\beta$ 42, etc.), and these $A\beta$ peptides are easily formed aggregates in cerebral amyloid angiopathy and AD brain.^{3,7} The $A\beta$ aggregation process will proceed through the formation of a polymorphic oligomeric nucleus, and then it initiates the formation of protofibrils and

followed by fibril elongation, and they individually show a range of cellular toxicities.⁸ Amyloid fibrils are larger, hydrophobic, and insoluble forms with toxic and cause neurotoxicity and dementia with common cytopathic effects that contribute to the pathogenesis of AD and another amyloidosis.^{9,10} Compounds, which can interfere with the aggregation process of the $A\beta$ peptide, which may lead to effective and potent therapeutics for AD. Here, we have

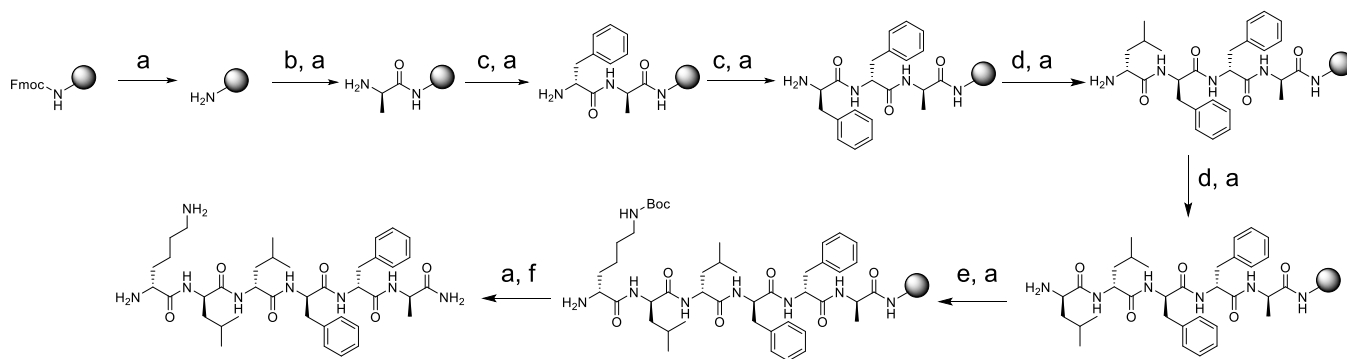
Received: October 20, 2022

Revised: January 6, 2023

Accepted: January 6, 2023

Published: February 15, 2023



Scheme 1. Synthetic Scheme for the Peptides by Using Rink Amide Resin Exemplified by Peptide NT-02^a

^aReagents and conditions: (a) 20% piperidine in DMF, 3 min (two times); (b) Fmoc-D-Ala-OH (10 equiv), HBTU (10 equiv), DIPEA (10 equiv), DMF, 7 min; (c) Fmoc-D-Phe-OH (5 equiv), HBTU (5 equiv), DIPEA (10 equiv), DMF, 7 min; (d) Fmoc-D-Leu-OH (5 equiv), HBTU (5 equiv), DIPEA (10 equiv), DMF, 7 min; (e) Fmoc-D-Lys (Boc)-OH (5 equiv), HBTU (5 equiv), DIPEA (10 equiv), DMF, 7 min; (f) 92.5% TFA, 2.5% water, 2.5% phenol, 2.5% 1,2-ethylenedithiol, 12 h.

Table 1. Sequence, HRMS, and HPLC Data of the Synthesized Peptides

s. no.	peptide sequence	molecular formula	mass		HPLC	
			calculated	obtained (M + H)	t _R (min)	purity (%)
1	H ₂ N-KLLFFAE-NH ₂	C ₄₄ H ₆₇ N ₉ O ₉	865.5062	865.6390	5.196	100
2	H ₂ N-KLLFFA-NH ₂	C ₃₉ H ₆₀ N ₈ O ₆	736.4636	737.7675	5.275	100
3	H ₂ N-KLLFF-NH ₂	C ₃₆ H ₅₅ N ₇ O ₅	665.4265	666.7092	5.298	100
4	H ₂ N-KLLF-NH ₂	C ₂₇ H ₄₆ N ₆	518.3581	519.3088	5.303	100
5	H ₂ N-LLFFAE-NH ₂	C ₃₈ H ₅₅ N ₆	737.4112	738.5652	5.301	100
6	H ₂ N-LLFFA-NH ₂	C ₃₃ H ₄₈ N ₆	608.3686	609.4024	5.280	100
7	H ₂ N-LLFF-NH ₂	C ₃₀ H ₄₃ N ₅	537.3315	538.5833	5.232	100
8	H ₂ N-LFFAE-NH ₂	C ₃₂ H ₄₄ N ₆	624.3271	625.3097	5.247	99.12
9	H ₂ N-LFFA-NH ₂	C ₂₇ H ₃₇ N ₅	495.2846	496.2403	5.156	100
10	H ₂ N-KLPFFAE-NH ₂	C ₄₃ H ₆₃ N ₉	849.4749	850.7135	5.201	100
11	H ₂ N-KLPFFA-NH ₂	C ₃₈ H ₅₆ N ₈	720.4323	720.6613	5.190	98.93
12	H ₂ N-KLPFF-NH ₂	C ₃₅ H ₅₁ N ₇	649.3952	650.2834	5.251	100
13	H ₂ N-LPFFAE-NH ₂	C ₃₇ H ₅₁ N ₇	721.3799	721.1677	5.203	100
14	H ₂ N-LPFFA-NH ₂	C ₃₂ H ₄₄ N ₆	592.3373	593.5271	5.178	99.58
15	H ₂ N-KLVFF-NH ₂	C ₃₅ H ₅₃ N ₇	651.4108	652.3820	5.222	98.98
16	Aβ ₄₂	NH ₂ - ¹ DAEFRHDSGYEVHHQKLVFFAEDVGSNKGAIIGLMVGGVVIA ⁴² -COOH				

focused on (i) developing the metabolic protease-stable peptide molecules having D-configuration, (ii) identifying the peptides which interact with the hydrophobic core residues which responsible for initial nucleus formation, and (iii) finally studying the effects of these metabolically stable peptides on β -sheet formation in vitro. The A β peptide is amphiphilic, with a hydrophobic C-terminal residue 29GAIIGLMVGGVVIA⁴² and the N-terminal (NT) residue 10YEVHHQKLVFFAEDV²⁴. The C-terminal residue inherently adopts β -sheet conformation and the NT residue 10YEVHHQKLVFFAEDV²⁴, which allows the existence of a dynamic equilibrium between α -helix and β -sheet conformation. The A β peptide will exist in two conformations depending upon the secondary structure adopted by the N-terminus domain and its effects on its rate of β -sheet formation.¹¹ The N-terminus amino acid residue 16KLVFF²⁰ is a key fragment, which plays an important role in the self-recognition of the parent A β peptide, and then leads to the formation and stabilization of β -sheet fibrils, but for the A β peptide self-recognition, 18Val is not completely necessary.¹² The alteration of the hydrophobic residue in the natural A β peptide structure shows the pipeline to the development of hydrophobic core-based β -sheet breakers for the therapy of AD.¹³ The substitution of

hydrophobic amino acids in the N-terminus hydrophobic fragment (KLVFF) of the natural A β peptide reduces the formation of the β -sheet followed by the polymerization of the A β peptide into aggregates.¹⁴ In the present study, our approach to generating β -sheet breakers, for this A β self-recognition hydrophobic core residue 16KLVFFAE²², was used to achieve specificity and good binding affinity¹⁵ but the replacement of a key amino acid residue (18Val which is responsible for β -sheet formation) by an amino acid which is unable to fit with the hydrophobic core residue and may not involve in the β -sheet formation. Here, we have developed a small library of NT peptide molecules with the replacement of this 18Val by using a hydrophobic amino acid, leucine, which can increase α -helix stabilization,¹⁶ and proline, which can stabilize the α -helix and disrupt the β -sheet structure effectively.¹⁷ The peptides with Leu and Pro in their backbone make the particular structure, and they may interfere with the full length of the A β peptide and prevent self-recognition and inhibit the β -sheet-based A β aggregate formation. From this library, we found that peptides NT-02, NT-03, and NT-13 are potent β -sheet breakers. These newly designed NT peptides not only alter A β self-assembly but also reduce the A β toxicity in vitro. These NT peptides show significant activity in various

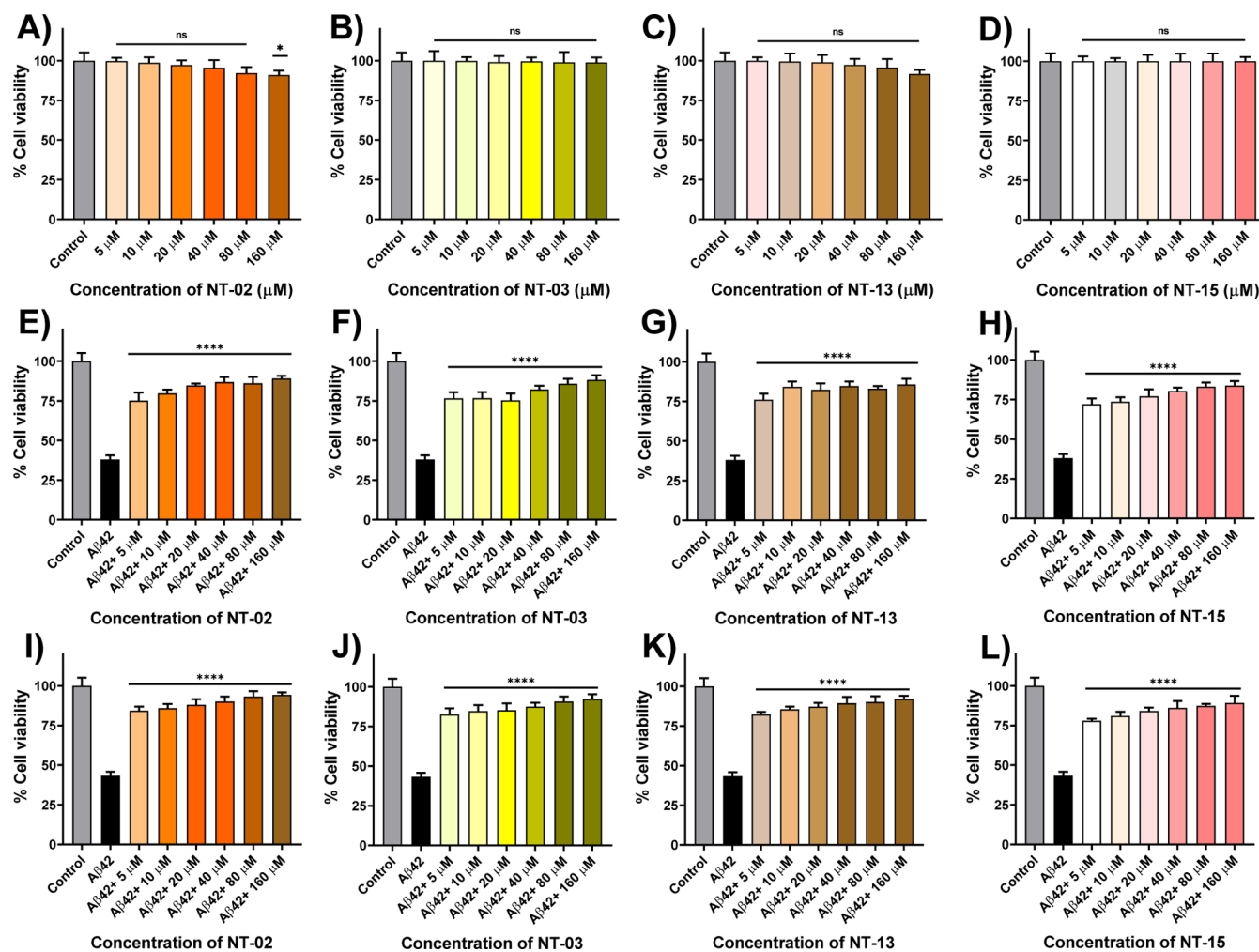


Figure 1. Cellular viability of peptides (A) NT-02, (B) NT-03, (C) NT-13, and (D) positive control NT-15 (KLVFF) in PC-12-derived neurons by using the MTT assay. Effects of NT peptides on the Aβ42 peptide-induced cytotoxicity in PC-12-derived neurons. (E) PC-12-derived neurons were treated with the Aβ42 peptide (5 μM) alone and Aβ42 peptide with (E) NT-02, (F) NT-03, (G) NT-13 peptide, and (H) positive control NT-15 for 24 h after which their ability to reduce MTT was measured. Cellular viability of PC12-derived neurons after being treated with Aβ42 aggregates (5 μM) alone and Aβ42 aggregates with (I) NT-02, (J) NT-03, (K) NT-13 peptides, and (L) positive control NT-15 for 24 h after which their ability to reduce MTT was measured. Error bars represent mean ± standard deviation (SD), n = 3. Statistical data were analyzed by a one-way ANOVA test by the multiple comparison tests (*p < 0.05, **p < 0.01, ***p < 0.001, ****p < 0.0001, vs Aβ42) using software (GraphPad Prism, ISI, San Diego, CA).

regions which (i) selectively interact with the N-terminus hydrophobic region of Aβ and interfere with the formation of Aβ aggregates, (ii) are nontoxic to PC-12 derived neurons, showing remarkable neuroprotection against Aβ-induced toxicity in PC-12 derived neurons, (iii) have good serum stability, and (iv) peptides easily cross the blood–brain barrier (BBB) in mice.

RESULTS AND DISCUSSION

Synthesis, Purification, and Characterization of Peptides

All the peptides (NT-01 to NT-14) were synthesized by using the solid-phase peptide synthesis (SPPS) method using Fmoc-protected rink amide resin. The synthetic scheme is described in Scheme 1. The conjugation of the peptide with fluorescein dye (5(6)-carboxyfluorescein) was achieved at the NT of the peptides to carry out the cellular uptake study. All the peptides were purified through RP-HPLC and characterized by high-resolution mass spectrometry (HRMS) and MALDI mass spectrometry (Tables 1 and S1, and Figures S7–S43).

MTT Cell Viability Assay

For the initial screening of newly synthesized NT peptides against Aβ peptide aggregation, we performed the MTT (3-(4,5-dimethylthiazol-2-yl)-2,5-diphenyltetrazolium bromide) cell viability assay to evaluate the effect of NT peptides against Aβ aggregation and Aβ-induced toxicity in PC-12-derived neuronal cells. PC-12 (rat pheochromocytoma cells) cells have been previously well-developed models for neuronal toxicity studies and to show their sensitivity to the toxic effects of Aβ aggregates.¹⁸ Reduction of MTT to formazan takes place in live cells by the NAD(P)H-dependent oxidoreductase enzyme, but in dead cells, this reduction process will not take place because of the absence of the NAD(P)H-dependent oxidoreductase enzyme; by this experiment, we can measure the cell proliferation and cellular viability after the treatment of the compound on PC-12 cells in drug screening.^{19,20} First, we checked the cellular toxicity of peptides. For this, we treated different concentrations (5, 10, 20, 40, 80, and 160 μM) of NT peptides with differentiated PC-12-derived neurons. The

results indicated that a maximum number of NT peptides did not show any toxic effect on the PC-12-derived neurons (Figures 1 and S1). However, only peptides NT-06, NT-07, and NT-08 showed 71.68, 42.54, and 50.07% of cell viability at a 160 μM concentration, respectively, as shown in Figure S1 and Table S2. Then, we check the neuroprotection capability of newly synthesized hydrophobic NT peptides against $A\beta_{42}$ peptide-induced toxicity in PC-12-derived neurons by performing the MTT cell viability assay. It has been described before that the amino acid residues $A\beta$ (16–20) (KLVFF) show strong activity against $A\beta$ toxicity and prevent fibril formation.¹⁴ In the MTT assay, KLVFF (NT-15) is taken as a positive control. The $A\beta_{42}$ -untreated PC-12-derived neurons were taken as 100% viable. First, PC-12-derived neurons were treated with the $A\beta_{42}$ monomer peptide alone and NT peptides with the $A\beta_{42}$ peptide and incubated for 24 h. Since formazan formation takes place by viable cells only. When the $A\beta_{42}$ peptide was treated alone, a reduction in the number of viable cells along with a decrease in the formation of formazan was observed, indicating cytotoxicity induced by the $A\beta_{42}$ peptide. However, NT-01, NT-02, NT-03, NT-04, NT-05, NT-06, NT-07, NT-08, NT-09, NT-10, NT-11, NT-12, NT-13, and NT-14 peptides showed 43.20, 75.13, 76.64, 73.46, 74.38, 62.61, 35.54, 44.35, 40.33, 50.19, 60.08, 36.10, 76.08, and 60.58% of cell viability against $A\beta_{42}$ -induced toxicity with 5 μM $A\beta_{42}$ and 5 μM NT peptides, respectively (1:1 ratio) (Figures 1E–G, S2, and Table S3). When PC-12-derived neurons were treated with the $A\beta_{42}$ peptide alone, the cells died and the cell viability was 38.05% only, followed by positive control KLVFF (NT-15) that showed a 72.08% cell viability (Figure 1H). Moreover, we checked for the inhibitory effects on the $A\beta_{42}$ peptide aggregation at different concentrations, 5, 10, 20, 40, 80, and 160 μM , of the NT peptide (Figures 1E–H and S2). The results show that the maximum number of NT peptides rescue the PC-12 neurons from $A\beta_{42}$ -induced toxicity. From the experimental results, peptides NT-02, NT-03, and NT-13 showed high neuroprotection against $A\beta_{42}$ -induced toxicity and showed a cell viability of nearly 85–90% by inhibiting the aggregation and reducing the neurotoxicity (Figure 1E–G). When compared with the positive control KLVFF peptide, the cell viability and neuroprotection of NT-02, NT-03, and NT-13 were higher, but those of the remaining peptides NT-01, NT-04, NT-05, NT-06, NT-07, NT-08, NT-09, NT-10, NT-11, NT-12, and NT-014 were less or nearly the same as those of the positive control. Furthermore, we incubated the NT peptides with $A\beta_{42}$ for 7 days with constant stirring at 37 $^{\circ}\text{C}$ to form fibrillary aggregates. Then, the fibrillary $A\beta_{42}$ aggregates were subjected to PC-12 derived neurons to check the fibrillary $A\beta_{42}$ aggregate-induced toxicity in PC-12 neuronal cells. Then, we performed the MTT assay, with results indicating that peptides NT-02, NT-03, and NT-13 were more potent than all other peptides (Figures 1I–K), showing a 94.30, 92.41, and 92.16% viability, respectively, at a 160 μM concentration. This MTT assay clearly shows that the peptides NT-02, NT-03, and NT-13 are highly potent and active against $A\beta$ peptide aggregation and protect the neurons from $A\beta$ -induced toxicity. Then, we checked the cellular uptake of our peptides using PC-12-derived neurons. For this, PC-12-derived neurons were treated with 5(6)-carboxyfluorescein-conjugated NT peptides. The experimental results show that (Figure 2) neurons were healthy in morphology, and cell bodies and dendrites were found to stain with green color 5(6)-carboxyfluorescein-

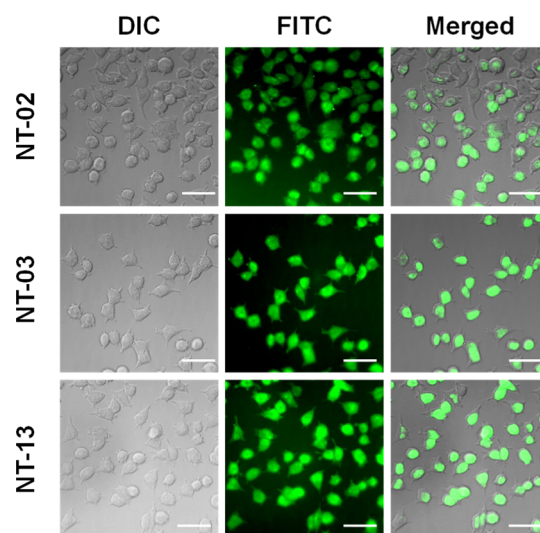


Figure 2. Cellular uptake images of 5(6)-carboxyfluorescein-attached NT-02, NT-03, and NT-13 peptides in differentiated PC-12-derived neurons reveal a significant cellular uptake. The scale bar corresponds to 50 μm .

conjugated NT-02, NT-03, and NT-13 peptides, and these outcomes suggest that our peptides show sufficient cellular uptake in the PC-12-derived neurons, and this opens the path to performing *in vitro* cellular studies.

Modulation of Neuronal Apoptosis

NT peptides protect the neurons from $A\beta_{42}$ -induced toxicity by preventing aggregation. Here, we assessed the neuronal toxicity by using the cell apoptosis assay. For this, PC-12-derived neurons were treated with $A\beta_{42}$ (10 μM) alone and $A\beta_{42}$ (10 μM) with NT-02, NT-03, and NT-13 peptides (10 μM) for 24 h. For the analysis of live cells and dead cells, we stained the neurons with Calcein AM and propidium iodide (PI). The reduction of apoptosis in PC-12-derived neurons by NT peptides was confirmed by using PI staining, which can stain late apoptotic cells and show red fluorescence. Figure 3 shows the effective rescue of PC-12-derived neurons from $A\beta_{42}$ induced apoptosis by NT peptides. The fluorescence intensity of PI (apoptosis cells) was quantified and is shown in Figure 4A. The $A\beta_{42}$ -only-treated neurons showed 31.04-fold apoptosis after 24 h of incubation, and NT-02, NT-03, and NT-13 peptides showed significant protection and rescued the neurons from apoptosis with a reduction to 2.84-, 6.21-, and 4.13-fold apoptotic cells, respectively. These results suggest that NT peptides are nontoxic in nature and insignificant apoptosis inducers.

ThT Assay

The $A\beta$ peptide has different morphological forms in the AD brain. The $A\beta$ peptide monomer can form higher-order assemblies ranging from the low molecular weight of dimers, trimers, and tetramers to higher-range molecular weight oligomers, protofibrils, and fibrils. $A\beta$ fibrils are insoluble and they induce membrane disruption, synaptic dysfunction, and finally neuronal death. Thioflavin-T (ThT) is a benzothiazole dye; it shows enhancement of fluorescence intensity upon binding to $A\beta$ fibril aggregates, and it is commonly used to monitor the $A\beta$ fibrillary aggregation, both *in vitro* and *in vivo*.²¹ Additionally, the fluorescence intensity of ThT indicates the quantity of $A\beta$ aggregates present in the solution.

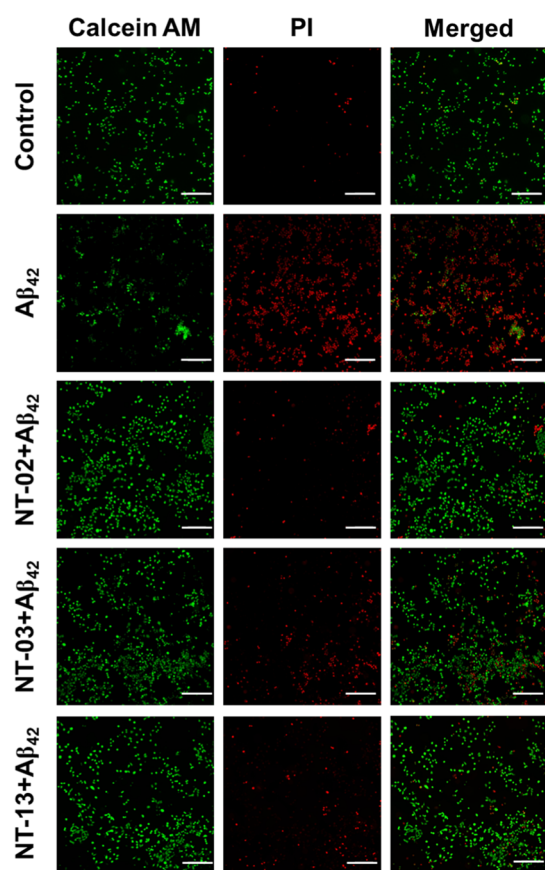


Figure 3. Cell apoptosis. Fluorescence images of differentiated PC-12-derived neuronal cells stained with Calcein AM and PI for normal and late apoptotic cell visualization. Initiation of apoptosis by $A\beta_{42}$ peptide treatment compared to the control and rescue by NT-02, NT-03, and NT-13 peptides. The scale bar corresponds to 200 μm .

The ThT assay was executed to evaluate the inhibition of $A\beta$ aggregation using all the peptides. In the ThT study, the control experiment $A\beta_{42}$ alone showed the increment of fluorescence intensity, but in the case of $A\beta_{42}$ incubated with NT peptides, we did not find the increment of fluorescence intensity. From the experimental results, all the designed peptides have the potential ability to interact with the $A\beta$ peptide and inhibit self-aggregation. First, we recorded the fluorescence intensity of the alone $A\beta_{42}$. Taking the $A\beta_{42}$ aggregation $A\beta_{42}$ alone as 100%, the % aggregates were calculated for the samples $A\beta_{42}$ treated with the NT peptides. For the positive control peptide, KLVFF (NT-15) was used. Figures 4B–D and S4 show the % of $A\beta_{42}$ aggregates present in the $A\beta_{42}$ peptide incubated alone, $A\beta_{42}$ with NT peptides, and $A\beta_{42}$ with KLVFF. From the ThT assay, the maximum of the NT peptides shows 45–60% inhibition at a concentration of 5 μM . However, peptides NT-02 (57.61%), NT-03 (54.26%), and NT-13 (48.41%) showed higher inhibition than the other peptides as well as a positive control NT-15 (41.87). Then, we executed the dose-dependent ThT assay with $A\beta_{42}$ peptide by using various concentrations of NT peptides. The positive control experimental results show that the % aggregation is 58.13, 55.02, 48.04, 39.18, 35.98, and 30.29%, but in the presence of peptide NT-02, the % aggregation is 42.39, 36.33, 29.77, 25.57, 22.14, and 21.04%, peptide NT-03 shows 45.74, 35.71, 25.34, 21.56, 20.63, and 19.37%, and peptide NT-13 shows 51.59, 35.61, 24.49, 23.15,

22.25, and 20.12% when $A\beta_{42}$ was incubated with various concentrations (5, 10, 20, 40, 80, and 160 μM) of NT peptides, respectively (Figures 4B–D and Table S5). This means that the peptides inhibited about 78.96, 80.63, and 79.88% of the $A\beta_{42}$ peptide aggregation at a 160 μM concentration of peptides NT-02, NT-03, and NT-13, respectively. This ThT assay was well supported by the MTT assay and clearly showed that NT-02, NT-03, and NT-13 peptides inhibited $A\beta_{42}$ peptide aggregation. Moreover, using the ThT assay, we also checked if the peptides NT-02, NT-03, and NT-13 were in a time-dependent manner against the inhibition of $A\beta_{42}$ peptide aggregation. Figures 4E–G shows that the $A\beta_{42}$ peptide with NT peptides and $A\beta_{42}$ alone. We can see that in the $A\beta_{42}$ peptide alone, there was a dramatic increment in the ThT fluorescence intensity that could be ascribed to the aggregation state of the $A\beta_{42}$ peptide. When the 12 h time represents the lag phase shows the absence of larger $A\beta_{42}$ aggregates. After 12 h, the dynamic increase in the fluorescence intensity corresponds to the growing phase. The fluorescence intensity reached maximum saturation after about 96 h. The saturated fluorescence intensity was taken as 100%. Then, % aggregation was calculated for peptides NT-02, NT-03, and NT-13, which showed 35, 46, and 31% at 96 h of incubation, respectively. The NT peptides were incubated with the $A\beta_{42}$ peptide, showing that the fluorescence intensity reached saturation at 72 h. Since the fluorescence intensity corresponded to the aggregation state of the $A\beta_{42}$ peptides, a complete reduction of fluorescence intensity was observed in the presence of peptides NT-02, NT-03, and NT-13. This indicates that NT peptides can interfere with the $A\beta_{42}$ peptide and in the self-assembly. In the meantime, the peptides showed their inhibitory effects on $A\beta_{42}$ aggregation even after a long-time incubation. Next, we performed an isothermal titration calorimetry (ITC) study to know the binding affinity of NT peptides with the $A\beta_{42}$ peptide. This study reveals that the binding affinities (K_a) of NT-02, NT-03, and NT-13 are about $2.25 \times 10^6 \pm 1.023 \times 10^5$, $(3.47 \pm 1.23) \times 10^6$, and $1.42 \times 10^5 \pm 3.42 \times 10^4 \text{ M}^{-1}$, respectively (Figure 5A–C). This result shows that peptides have a good binding affinity with the $A\beta_{42}$ peptide. From the ThT fluorescence results, it was found that the peptides NT-02, NT-03, and NT-13 are more potent than all other peptides. The ThT experimental results further support the results we saw in the MTT assay.

Molecular Docking Studies

According to the amino acid analysis of the $A\beta$ peptide by the Chou–Fasman²² and Garnier–Osguthorpe–Robson methods,²³ the probability of β -sheet conformation is higher in the $A\beta$ peptide within the regions that consist of the hydrophobic C-terminal region after residue 28 (residues 29–42) and the NT region (residues 10–24). The structure of the NT domain is important for $A\beta$ fibril formation, and this region will show a dynamic equilibrium between the α -helix and β -sheet conformations of the $A\beta$ peptide.²⁴ In the hydrophobic segment in the C-terminus of the $A\beta$ peptide, invariably, it adopts β -sheet conformation in aqueous solutions at independent pH and various temperatures. However, the N-terminus hydrophobic domain will show different conformations depending on the conditions. While at pH = 1–4 and greater than pH = 7, the $A\beta$ peptide will show the α -helix conformation, at pH = 4–7, it rapidly forms and shows the β -sheet conformation.^{25–27} Moreover, the $A\beta$ peptide will show

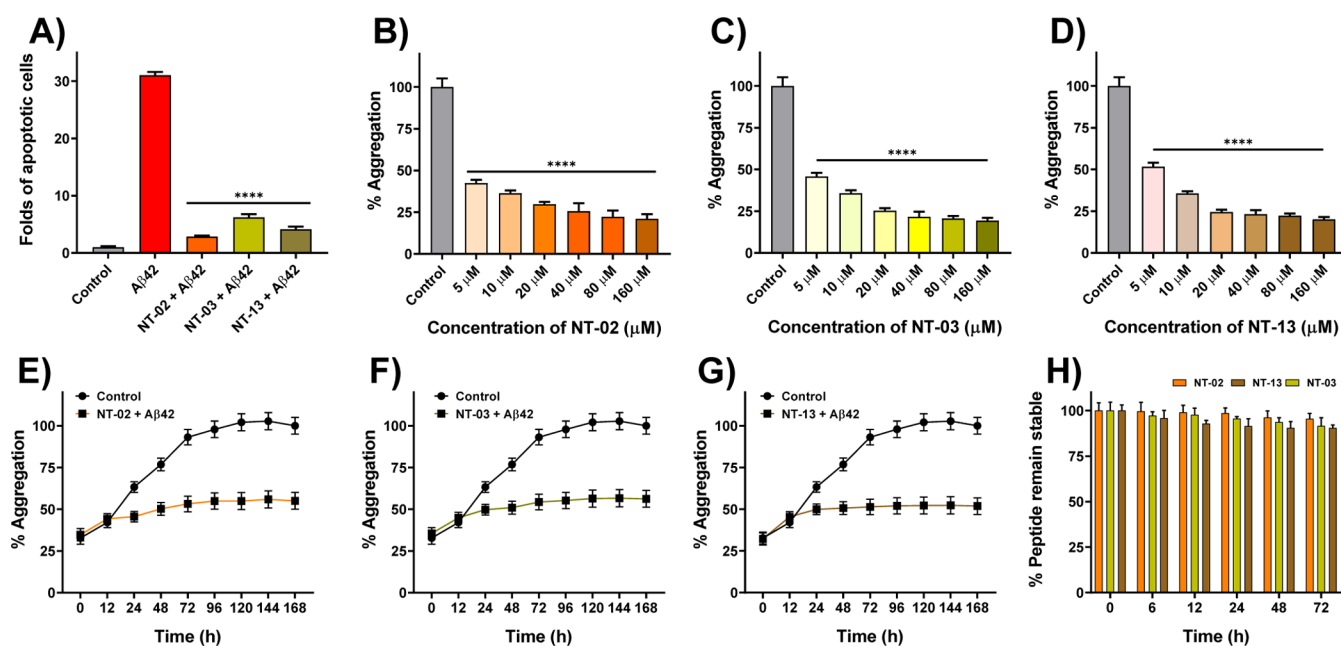


Figure 4. (A) Quantification of percentage apoptotic cells of different treatments shows the significant rescue of cells from Aβ42-induced apoptosis by NT-02, NT-03, and NT-13 peptides. Effects of NT peptides on Aβ42 aggregation measured by the ThT fluorescence assay. (B) Peptides NT-02, (C) NT-03, and (D) NT-13 in Aβ42 aggregation. The control sample represents the Aβ42 peptide (5 μM) alone. (E–G) Effects of peptides NT-02, NT-03, and NT-13 on Aβ42 aggregation for 7 days. Aβ42 (5 μM) and peptide at a 10 μM concentration. Control sample represents the Aβ42 peptide (5 μM) alone. (H) Serum stability of NT peptides in human serum up to 24 h. Error bars represent mean ± standard deviation (SD), $n = 3$. Statistical data were analyzed by a one-way ANOVA test by the multiple comparison tests (* $p < 0.05$, ** $p < 0.01$, *** $p < 0.001$, **** $p < 0.0001$, vs Aβ42) using software GraphPad Prism (ISI, San Diego, CA).

the α -helix when the membrane mimics solvents that promotes an intramolecular hydrogen bonding with the Aβ peptide. Because of this, the Aβ peptide will exist in two conformations depending upon the secondary structure adopted by the N-terminus domain. Here, we perform molecular docking studies so that we can see how our peptide will interact with Aβ peptides and how it can reduce the β -sheet formation followed by reducing the Aβ aggregate formation. Molecular docking studies have been widely used for studying protein–ligand interactions and their binding modes. Here, we carried out molecular docking studies with the Aβ42 monomer structure (PDB ID: 1Z0Q)²⁸ to find out the binding modes of our peptides with Aβ42. The molecular docking studies results show that there are multiple binding sites in Aβ42 for the binding of peptides. However, the most favorable binding site is shown in Figure 5D–F. From the docking study, all the peptides have selectively binding interactions with N-terminus hydrophobic region residues of Aβ42. Peptides NT-02 and NT-03 were bound with the Aβ42 peptide (PDB ID: 1Z0Q) at Glu11, His14, Gln15, and Asp23 and Glu3, Asp7, and His14 through hydrogen bonding interaction. Peptide NT-13 shows hydrogen bonding interaction with His14 and Tyr10 residues. The molecular docking studies reveal that the peptides NT-02, NT-03, and NT-13 can interact with the N-terminus region of the Aβ42 peptide and then prevent the self-recognition and β -sheet formation, followed by aggregation of the Aβ42 peptide. These results indicate that the N-terminus hydrophobic core residues 10 to 24 of Aβ are crucial for the formation of β -sheets. This result further supports the results we saw in the MTT assay and ThT assay.

Fourier Transform Infrared Spectroscopy Studies

The results from MTT assay, ThT assays, and docking studies attracted us to further study the peptides. The molecular

docking experiment results show that peptides have a binding interaction at the N-terminus region of the Aβ42 peptide. When the peptide binds to the N-terminus region of Aβ42, it may reduce the stabilization of β -sheet conformation, followed by its aggregation. Here, we check the interaction of peptides with Aβ42 and their antiaggregation effect by a reduction in β -sheet formation by Fourier transform infrared (FTIR) spectroscopy.^{29,30} Moreover, the Aβ42 peptide will show a secondary structure like the α -helix and β -sheet. FTIR spectroscopy provides information about the secondary structure content of the Aβ42 peptide in a solution. The Aβ42 contains amide bonds and shows a characteristic absorption in the infrared (IR) spectrum. The C=O and N–H bonds both are involved in the hydrogen bonding interaction between the different elements of the secondary structure of Aβ42. The α -helix and β -sheet structure were resolved by systematically the shape of the C=O amide bond present in the secondary structure of Aβ42. The amide bond C=O has its characteristic absorption frequency in the IR region, α -helix (1640–1660 cm^{-1}), β -sheet (1610–1640 cm^{-1}), and random coil (1640–1650 and 1660–1685 cm^{-1}). The Aβ peptide is self-aggregated and forms β -sheet fibrils, which are toxic. Here, we checked the effect of our newly designed NT peptides against Aβ peptide aggregation to form β -sheet fibrils. First, we checked the Aβ peptide secondary structure content by subjecting the Aβ peptide alone to FTIR spectroscopy without any incubation (Figure 6A). The IR spectrum shows the C=O amide stretching frequency at 1642.84 cm^{-1} , which indicates that the Aβ peptide was in the form of α -helix. Then, we incubated the Aβ42 peptide alone for 7 days and then subjected it to FTIR spectroscopy. The IR spectrum (Figure 6B) shows the C=O amide bond stretching frequency at 1638.89 cm^{-1} , and it clearly shows the formation

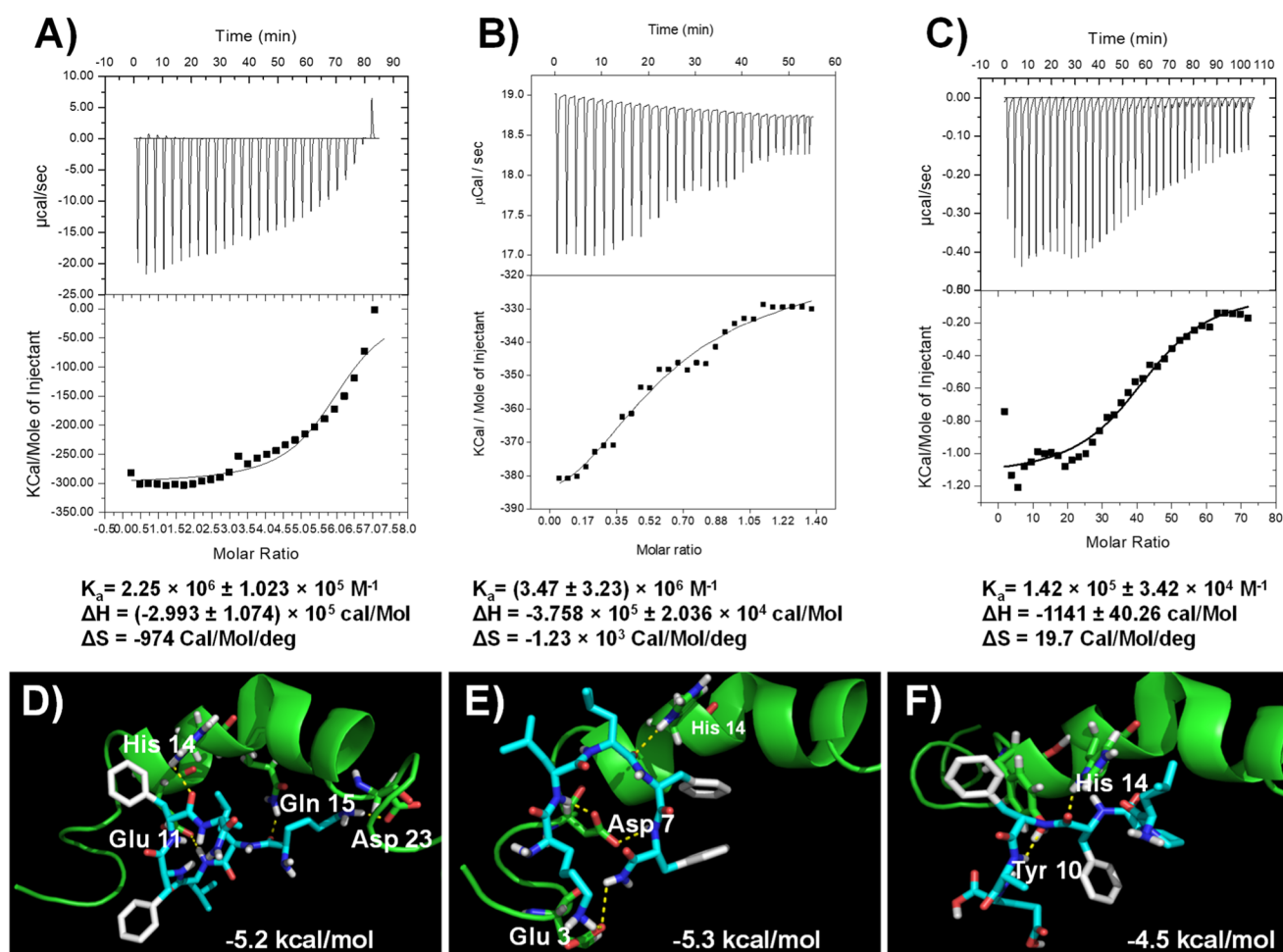


Figure 5. ITC experiment of NT peptides showing interaction with the Aβ42 peptide. (A) NT-02 peptide shows an affinity of $2.25 \times 10^6 \pm 1.023 \times 10^5 \text{ M}^{-1}$, (B) NT-03 peptide shows an affinity of $(3.47 \pm 1.23) \times 10^6 \text{ M}^{-1}$, and (C) NT-13 peptide shows an affinity of $1.42 \times 10^5 \pm 3.42 \times 10^4 \text{ M}^{-1}$. Molecular docking images of NT peptides with the Aβ42 peptide (PDB ID: 1Z0Q). (D) Docking studies of the NT-02 peptide with the Aβ42 peptide show H-bonding interaction with a -5.2 kcal/mol binding energy. (E) Docking studies of NT-03 with Aβ42 and showing H-bonding interactions with -5.3 kcal/mol binding energy. (F) Docking studies of NT-13 with Aβ42 and showing H-bonding interaction with a -4.5 kcal/mol binding energy.

of β-sheets. By these two IR spectra, we have confirmed the formation of β-sheets after 7 days of incubation of the Aβ peptide. After these, we checked the effect of our peptides if they can or cannot prevent the formation of β-sheets. Then, we incubated the Aβ peptide with our newly designed peptides NT-02, NT-03, and NT-13; the IR spectrum (Figure 6C–H) did not show the β-sheet characteristic peak in the range from 1610 to 1640 cm^{-1} , and IR spectra indicated that the solutions did not contain the β-sheet content, which means that the peptides inhibited β-sheet formation in the solution. When Aβ42 was treated with NT-02 and NT-13, Aβ42 was in the form of α-helix, observing peaks at 1642.76 and 1645.94 cm^{-1} , respectively, but when Aβ42 was treated with NT-03, it was in the form of a random coil by observing a peak at 1699.71 cm^{-1} . The results of FTIR spectroscopy show that peptides can prevent the self-recognition of parent peptides by binding at the N-terminus region and stabilizing the α-helix conformation and disrupting the β-sheet structure formation followed by reducing the Aβ induced toxicity. This means that our designing concept of the NT strategy is efficient and they bind with the NT region of the Aβ42 peptide and increase α-helix stabilization and inhibit β-sheet-based Aβ aggregate formation. These FTIR spectroscopy results further well

support the results we saw in the molecular docking studies by inhibition of fibril aggregation by binding at the N-terminus of the Aβ42 peptide and neuroprotection effects in PC-12-derived neurons and the results seen in the ThT assay.

Circular Dichroism Spectroscopy Studies

In the aqueous solution (pH = 7), the Aβ42 peptide adopts a structure as a mixture of α-helix, β-sheet, and random coil, and when it forms Aβ aggregates, the confirmations will be in the form of the β-sheet structure. Here, we analyzed the effect of our peptides on the formation of fibrillary β-sheets by using circular dichroism (CD) spectroscopy. CD spectroscopy is a technique that is widely used for the quantitative identification of structural aspects of proteins and peptides.³¹ The Aβ42 peptide bonds are optically active, and the ellipticity they exhibit may change based on the confirmation of the peptide bond. The secondary structure of proteins can be analyzed by CD spectroscopy by using the far ultraviolet region (far UV 180–260 nm). The protein secondary structural conformations (β-sheet, α-helix, and random coil) have characteristic spectra; on the basis of the unique spectra, protein structure analyses may be done. We performed CD spectroscopy to analyze the effect of our NT peptides on the secondary

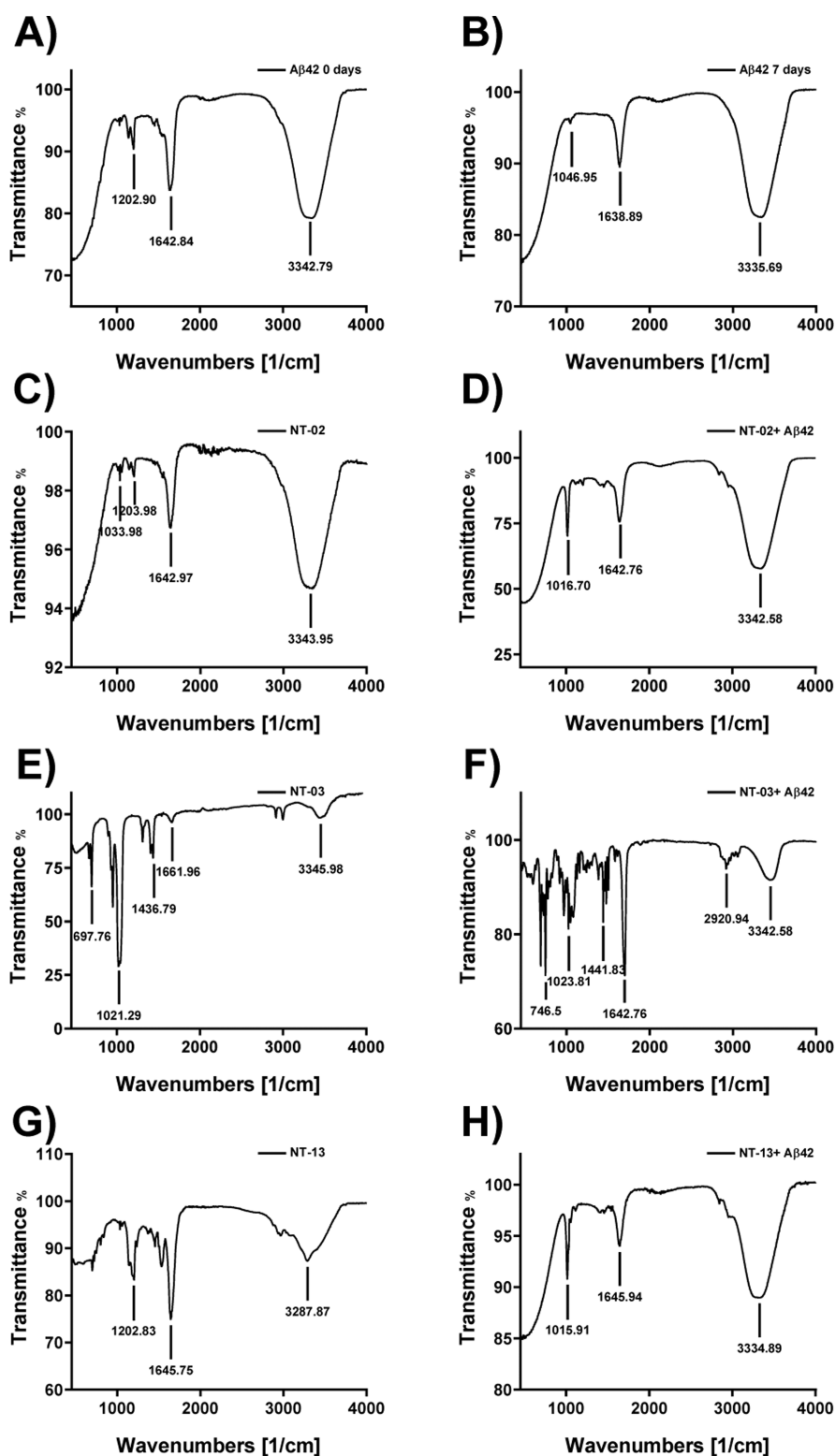


Figure 6. Analysis of β -sheet content by FTIR spectroscopy. FTIR spectrum of the (A) $A\beta$ 42 peptide alone for 0 day incubation. The spectrum shows the $A\beta$ 42 peptide in α -helix conformation. (B) $A\beta$ 42 peptide alone upon 7 days of incubation. The spectrum shows that the $A\beta$ 42 peptide converted into β -sheet conformation. (C,E,G) FTIR spectrum of peptide NT-02, 03, and 13 alone for 7 days of incubation. The spectrum shows that NT peptides in α -helix conformation. (D,F,H) FTIR spectrum of $A\beta$ 42 with NT-02, 03, and 13 for 7 days of incubation. The spectrum shows the $A\beta$ 42 peptide in α -helix conformation.

structural conformation changes of the $A\beta$ 42 peptide by observing the residual molar ellipticity at 217 nm. The negative ellipticity at 217 nm indicates the β -sheet content in proteins and peptides, and the deep negative ellipticity will increase at

217 nm as the content of the β -sheet increase. For this, we incubated the $A\beta$ peptide with three different concentrations (5, 10, and 20 μ M) of NT peptides for 7 days and the secondary structure was analyzed by CD spectroscopy. First,

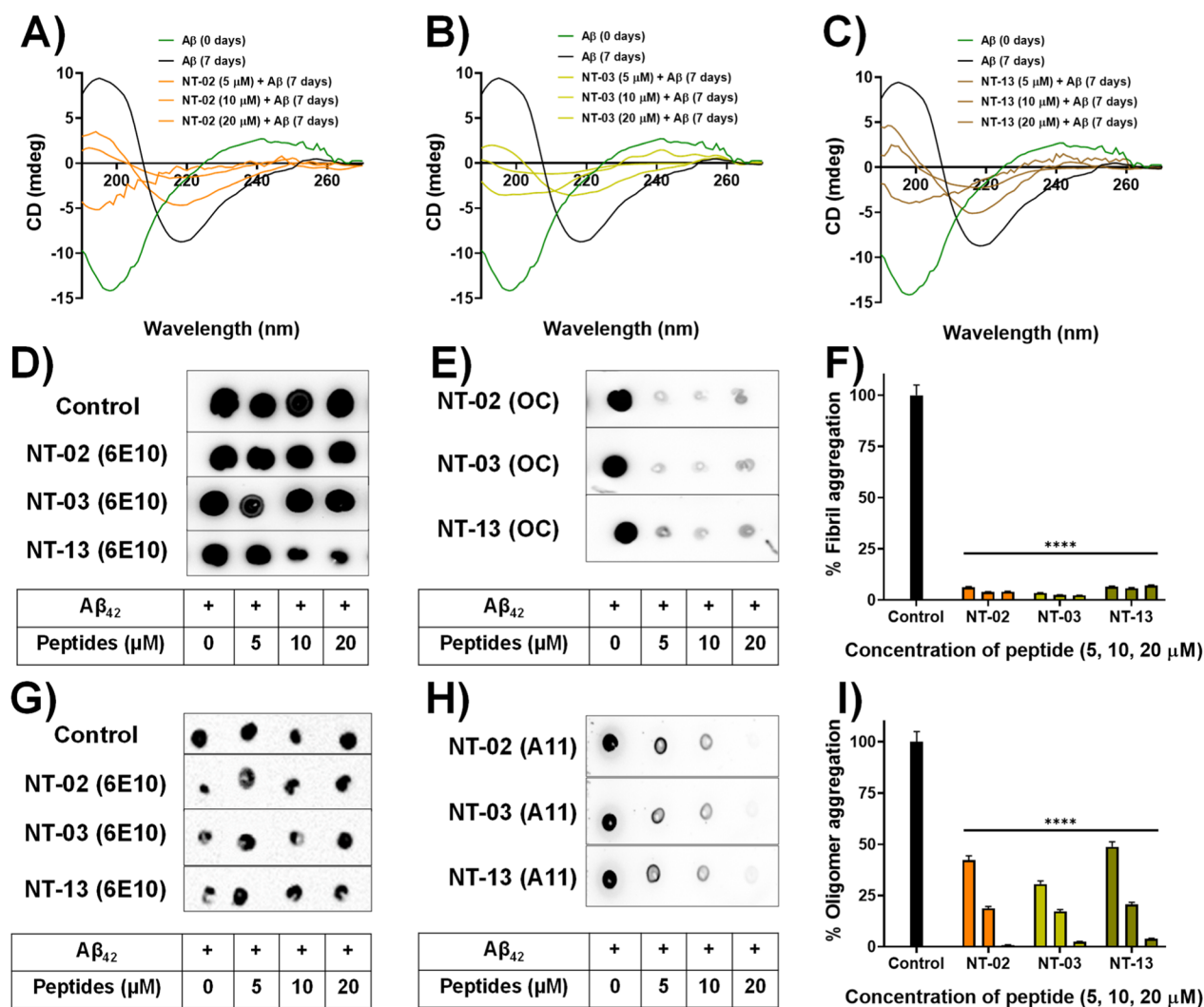


Figure 7. CD spectroscopic studies showing β -sheet content and the inhibitory effects of peptides (A) NT-02, (B) NT-03, and (C) NT-13. CD spectra show the $A\beta_{42}$ sample at $t = 0$ h (green), and the $A\beta_{42}$ sample at $t = 7$ days (black). Dot blot assay for monitoring $A\beta_{42}$ aggregation. (D) Dot blot image for $A\beta_{42}$ content detected by 6E10. (E) Dot blot image for $A\beta_{42}$ fibrillary aggregation inhibition in the presence of NT peptides detected by OC. (F) Bar diagram of $A\beta_{42}$ fibrillary aggregation inhibition by NT peptides. (G) Dot blot image for $A\beta_{42}$ content detected by 6E10. (H) Dot blot image for $A\beta_{42}$ oligomeric aggregation inhibition in the presence of NT peptides detected by A11. (I) Bar diagram of $A\beta_{42}$ oligomer inhibition by NT peptides. Error bars represent mean \pm standard deviation (SD), $n = 3$. Statistical data were analyzed by a one-way ANOVA test by the multiple comparison test (* $p < 0.05$, ** $p < 0.01$, *** $p < 0.001$, **** $p < 0.0001$, vs control) using software (GraphPad Prism, ISI, San Diego, CA).

we analyzed the secondary structure of the $A\beta_{42}$ peptide alone at 0 days of incubation and we found negative ellipticity at 197 nm which means that $A\beta_{42}$ is in a random coil. Figure 7A–C shows the peak (green color) negative ellipticity at 197 nm. Then, we incubated the $A\beta_{42}$ peptide alone for 7 days and analyzed the secondary structure, and the CD spectrum showed negative ellipticity at 217 nm. Figure 7A–C shows the peak (black color) negative ellipticity at 217 nm. This means that $A\beta_{42}$ forms the β -sheet structure after 7 days of incubation. Then, we incubated NT peptides with the $A\beta_{42}$ peptide for 7 days and analyzed the effect of the NT peptide on β -sheet formation. The results indicate that in the presence of our NT peptides, a reduction in β -sheet content was observed by a reduction in negative ellipticity at 217 nm and an increase in the random coil content was observed upon increasing the negative ellipticity at 197 nm. Figure 7A–C shows negative ellipticity at 217 nm by order of $A\beta_{42}$ alone and $A\beta_{42}$ with NT peptides after incubation for 7 days. CD spectroscopy

reveals that the peptides can interact with $A\beta_{42}$ and prevent the formation of β -sheet formation, followed by aggregation of the $A\beta_{42}$ peptide.

Dot Blot Experiment to Monitor the Inhibition of $A\beta$ Aggregation

Furthermore, we move toward a blotting experiment to confirm the inhibition activity of peptides NT-02, NT-03, and NT-13. In this dot blot assay, we have used three different antibodies 6E10, OC, and A11 for the detection of a different form of the $A\beta$ peptide. Antibody 6E10 can bind to all kinds of $A\beta$ peptides like monomer, oligomer, and fibril aggregates and gives a positive trend; because of this, we used 6E10 as a control experiment to detect the $A\beta$ peptide content in the sample. For the specific detection of an oligomeric form of amyloid species content antibody A11 and for the detection of amyloid fibril aggregates, we used antibody OC.³² First, the $A\beta_{42}$ peptide was incubated alone and $A\beta_{42}$ with different

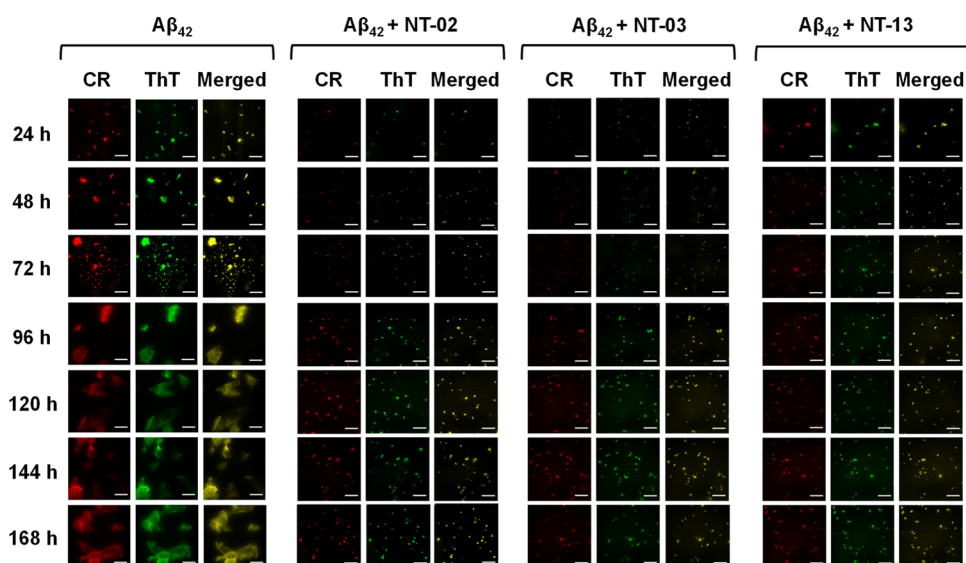


Figure 8. CR and ThT binding to $A\beta_{42}$ aggregates. Fluorescence microscopical images show the presence of $A\beta_{42}$ aggregates in all samples. Fluorescence microscopic images of $10\ \mu\text{M}$ $A\beta_{42}$ peptide in the presence of $1\ \mu\text{M}$ CR (column 1) and ThT (column 2). Images clearly indicate that NT peptides inhibit the formation of $A\beta_{42}$ aggregates. The scale bar corresponds to $200\ \mu\text{m}$.

concentrations (5, 10, and $20\ \mu\text{M}$) of NT peptide for the oligomer and fibril aggregate formation, separately. After incubation of the $A\beta$ peptide samples, the samples were spotted on three different nitrocellulose membranes. Then, the membranes were treated with three respective primary antibodies and secondary antibodies. Then, the chemiluminescence intensity of the spots on the membrane was measured. Here, we checked the antibody 6E10 staining of all the incubated samples. Since the 6E10 antibody detects all forms of $A\beta$. The experimental results clearly showed that all the samples have $A\beta$ peptide content indicated by the spot observed on the antibody 6E10-treated membrane. Figure 7D shows the $A\beta$ content in fibril aggregate samples, and Figure 7G shows $A\beta$ in oligomeric aggregate samples. Then, we checked the effect of the NT peptide on the formation of $A\beta_{42}$ aggregates, and the experimental results show that the $A\beta_{42}$ peptide alone formed the oligomers and fibrils, which are detected by antibodies A11 and OC with high intensity (Figure 7H,E). However, in the case of the $A\beta_{42}$ peptide with the NT peptide, a drastic reduction of spot intensity was observed (Figure 7H,E). When $A\beta_{42}$ was incubated with a $20\ \mu\text{M}$ concentration of NT peptides, the formation of oligomers and fibrils was completely inhibited and the spot completely disappeared. The spot intensity of the control sample with $A\beta_{42}$ alone was taken as 100%, and % inhibition was calculated for the samples treated with the NT peptides. Subsequently, the percentage of $A\beta$ aggregates in each test peptide was calculated by using the formula: % aggregates = $\left\{ \frac{\text{intensity of the test spot}}{\text{intensity of the control spot}} \right\} \times 100$. The bar diagram showed (Figure 7F,I) the % of aggregates present in the samples when compared with the control. This dot blot experiment clearly shows the anti-amyloid aggregation effect of NT peptides against the $A\beta_{42}$ peptide.

Microscopic Examination of the $A\beta_{42}$ Aggregation Process

It is well known that the formation of $A\beta$ fibril aggregates occurs by a nucleation-dependent elongation mechanism. However, because of the insufficient analytical methods, the detailed structural features of various intermediates in the

fibrillation pathway, including the initial structure and mechanism of nucleus formation, remain elusive. The fluorescent dyes ThT and Congo red (CR) are supposed to be used for specific imaging of the fibrillary structure. Here, we check the effect of the NT peptide on the fibrillation rate of the $A\beta$ peptide by using the microscopic examination. For this, we incubated the $A\beta$ peptide ($10\ \mu\text{M}$) solution alone and the $A\beta$ peptide ($10\ \mu\text{M}$) with NT peptides ($10\ \mu\text{M}$) for 7 days. For the visualization of $A\beta$ peptide aggregation and the effect of NT peptides on its rate formation, we took aliquots from incubated solutions every 24 h and analyzed them by fluorescence microscopy. The incubated solutions were taken, and to this fluorescent dye, ThT or CR was added and kept aside for 1 min in the dark condition. Then, the fibrillary structures were imaged by fluorescence microscopy in the presence of the fluorescent dyes ThT and CR (Figure 8). The images clearly show the progression of $A\beta$ fibrillary aggregates when the $A\beta$ peptide is incubated alone. In the case of the $A\beta_{42}$ peptide alone, fluorescence spots were observed after 24 h of incubation. Then, a drastic increase after 72 h was observed and spots became highly fluorescent with an increase in the aggregation of the $A\beta_{42}$ peptide. After 92 h, saturation was observed and the $A\beta_{42}$ peptide showed mature fibrils with high fluorescence intensity. However, when the $A\beta$ peptide was coincubated with NT peptides, the progression of $A\beta$ aggregates was reduced and images clearly showed that NT peptides inhibited $A\beta$ fibrillation. In the case of NT peptides, fluorescent spots were observed at 24 h of incubation, but they were very less compared to $A\beta_{42}$ alone, and after 96 h, the fluorescent spots were saturated and they were very less and small in size when compared with the $A\beta_{42}$ peptide alone. The fluorescence microscopy images well support the above in vitro assays.

High-Resolution Transmission Electron Microscopy Studies

Transmission electron microscopy (TEM) provides detailed images of the macromolecular structures by passing an electron beam through the sample such that light will be absorbed and scattered and it produces contrast and images. TEM is a

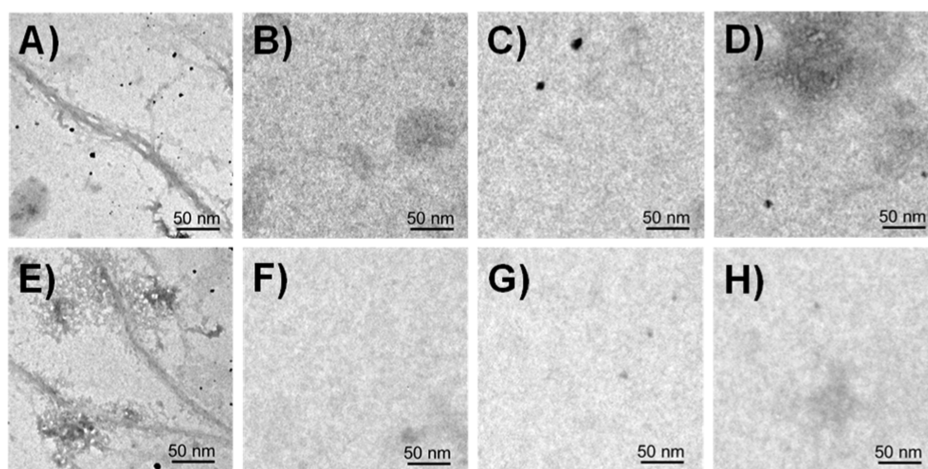


Figure 9. HR-TEM images. (A,E) $A\beta_{42}$ peptide fibrils after 7 days of incubation of $A\beta_{42}$ alone at 37 °C. Absence of the fibril structure after coincubation of the $A\beta_{42}$ peptide with (B) NT-02, (C) NT-03, and (D) NT-13 peptides at 37 °C for 7 days. Peptides (F) NT-02, (G) NT-03, and (H) NT-13 incubated alone for 7 days, and no fibril formation was observed.

pivotal tool widely used to identify the presence of $A\beta_{42}$ fibrils and study their morphology and size. Here, we used high-resolution-TEM (HR-TEM) microscopy to visually investigate the effects of NT peptides on the morphology, size, and distribution of $A\beta_{42}$ aggregates. For the control experiment, $A\beta_{42}$ was incubated alone for 7 days at 37 °C. After incubation of the $A\beta_{42}$ peptide, we observed numerous long thick rod-like cylindrical fibrils. Figure 9A,E shows the fibril aggregation state of the $A\beta_{42}$ peptide. However, after incubation of $A\beta_{42}$ with NT peptides, outstanding changes were observed in the morphology and distribution of the $A\beta_{42}$ peptides. The aggregates were completely disappeared when the $A\beta_{42}$ peptide incubated with NT peptides (Figure 9B–D), and NT peptides did not form any aggregates and fibrils when incubated alone under the same conditions (Figure 9F–H). All these results again prove that our NT peptides play a key role in the $A\beta_{42}$ aggregation process and prevent the formation of higher-order assemblies.

Serum Stability Studies of NT Peptides

All the above studies indicate that peptides NT-02, NT-03, and NT-13 show a significant potential effect against $A\beta$ aggregation and protect neuronal cells from $A\beta$ -induced toxicity. However, any therapeutics designed for targeting the brain need to be stable in the physiological conditions and it should cross the BBB. For this, we check the stability of peptides in the human serum and find out that the peptides are potential candidates for performing in vivo experiments. Here, we studied the stability of peptides in human serum solution up to 72 h at 37 °C, and at different time intervals, aliquots were taken out from the incubated solution and we checked the percentage of safe peptides present in serum by using reverse-phase high-performance liquid chromatography (RP-HPLC). The HPLC data clearly shows that our peptides were stable in human serum solution and show 95.47, 91.57, and 90.44% of the intact peptide remaining in the serum after 72 h of incubation (Figure 4H) of NT-02, NT-03, and NT-13 respectively. Finally, our peptides show good stability in serum and this indicates that peptides have a greater bioavailability in physiological conditions. This means that the cleavage site of the peptide by serum protease was changed by using D-amino acid and increased the stability of the peptide in the serum.³³ These NT peptides are potential candidates for evaluation in

an animal model and for the development of anti-AD therapeutics.

BBB Crossing Studies

The brain has a natural barrier called the BBB; it helps to preserve the homeostasis of the brain's internal environment. It is made of neuronal cells, astrocytes, pericytes, and brain capillary endothelial cells. The tight connections between brain capillary endothelial cells prevent the transport of paracellular substances from blood to the brain. Therefore, more than 98% of organic small molecules do not cross the BBB. Therefore, a BBB crossing experiment was performed to check whether NT peptides can penetrate the BBB or not. We performed the BBB penetration test by following a previously well-established procedure.³⁴ Here, the peptides were injected intraperitoneally, and after 6 h, the mice were sacrificed through transcardial perfusion. The brains were collected and homogenized in an acetonitrile solution. Then, homogenized solutions were inspected by HRMS. The mass spectrum (Figure S5) shows the molecular mass peak of our peptides; as a negative control, sucrose was used, and we did not find the molecular peak in the mass spectrum. This BBB penetration experiment clearly shows that our peptides cross the BBB and show good biostability, which means that they have a greater potential in anti-AD drug development.

CONCLUSIONS

In summary, our newly designed proteolytically stable NT peptides were synthesized by replacing the hydrophobic amino acid 18Val with proline and leucine. By the evaluation of these peptides as an anti- $A\beta$ aggregating agent in vitro and in vivo experiments, we identified the peptides NT-02, NT-03, and NT-13, which are more potent than the other peptides are more potent than the other peptides. These NT peptides reduce $A\beta$ fibrillation in the range of 60–80% observed in the ThT assay. In the cellular system, these peptides are noncytotoxic and show a significant neuroprotection effect (85–90%) from $A\beta$ -induced toxicity and protects the neurons from $A\beta$ -induced apoptosis. Moreover, the effect of peptides on the formation of the β -sheet structure was analyzed by FT-IR and CD spectroscopies, and inhibition of aggregate formation was observed by fluorescence microscopy and HR-TEM electron microscopic images. Finally, these peptides NT-

02, NT-03, and NT-13 can cross the BBB, have significant stability in serum, and maintain healthy morphology of PC-12-derived neurons. From above, all the results suggest that proteolytically stable peptides could be a potential lead for further drug development against anti-AD and opens a new opportunity for treatment against AD.

EXPERIMENTAL SECTION

General Information

All the Fmoc-protected amino acids, Fmoc-D-Lys (Boc)-OH ($\geq 98\%$), Fmoc-D-Leu-OH ($\geq 99.5\%$), Fmoc-D-Val-OH ($\geq 98\%$), Fmoc-D-Phe-OH ($\geq 99.8\%$), Fmoc-D-Ala-OH ($\geq 99.5\%$), Fmoc-D-Glu (OtBu)-OH ($\geq 99.5\%$), and Fmoc-D-Pro-OH ($\geq 99.5\%$), and Rink Amide AM resin were purchased from Novabiochem (Merck, Germany). All chemicals including *N,N*-diisopropylethylamine (DIPEA), piperidine, 1,1,1,3,3,3-hexafluoroisopropanol (HFIP), 2,4-ethanedithiol, phenol, trifluoroacetic acid (TFA), 5(6)-carboxyfluorescein, and 3-[bis(dimethylamino)methyl]carbonyl-3H-benzotriazole-1-oxide hexafluorophosphate (HBTU) were purchased from Sigma-Aldrich and used without further purification unless specified. All the solvents including *N,N'*-dimethylformamide (DMF), methanol, acetonitrile (ACN), dichloromethane (DCM), and diethyl ether were purchased from Merck (Germany) and used for synthesis. All the solvents were of analytical grade and used without further purification unless otherwise stated. 3-(4,5-Dimethylthiazol-2-yl)-2,5-diphenyltetrazolium bromide (MTT), cell culture-grade DMSO, and Dulbecco's modified Eagle's medium (DMEM) were purchased from Sigma-Aldrich. $A\beta$ (1–42) was purchased from Autotec (Sweden). Human recombinant nerve growth factor (NGF) was purchased from Sigma (St. Louis, MO, USA), and anti-NGF was obtained from Abcam. Primary antibodies 6E10, A11, and OC were obtained from Bio Legend, Thermo Scientific, and Millipore, respectively. Nitrocellulose membranes were obtained from Merck Millipore. The fluorescence spectra were recorded using a Photon Technology International (PTI) Quanta Master fluorometer QM-40. RP-HPLC (Waters 1290 Infinity II Prep LC model using a Phenomenex TM column, LC-18, 250 \times 21.2 mm, 10 μ m) which was used for the purification of peptides and characterized for identity by HRMS and MALDI mass spectroscopy. Mass spectra were obtained using Agilent, G6530 Q-TOF HRMS, Applied Biosystems MDS SCIEX, and MALDI TOF/TOF analyzer (4800) mass spectrometer.

Synthesis of NT Peptides

All the peptides were synthesized by the SPPS method using Fmoc-protected rink amide resin in our laboratory. For the synthesis of peptides, we used 200 mg of Fmoc-protected rink amide resin in a reaction vessel and swelled the resin overnight in DMF/DCM (5 mL/5 mL) solvents at 4 °C. After 12 h of incubation, the reaction vessel was taken out and kept outside to bring it to room temperature. For the synthesis of peptides, we used Fmoc-protected D-amino acids. For the coupling of amino acid Fmoc-protected rink amide resin was deprotected with 20% piperidine in DMF and first amino acid was coupled to the resin was performed. Then, five equivalent Fmoc-protected amino acids were taken, five equivalents of DIPEA, and five equivalent HBTU were used as an activator base and DMF was used as a solvent in the CEM microwave peptide synthesizer (Liberty 1). All the amino acids were coupled successively and followed by Fmoc-deprotection was done by using 20% piperidine in DMF. After coupling of amino acids to resin and deprotection of amino acids after attaching them to resin washed by DMF and DCM solvents. All the fragment sequences were synthesized by the same protocol. Cleavage of prepared peptides from the resin was done by 92.5% TFA, 2.5% Milli Q water, 2.5% phenol, and 2.5% EDT (1,2-ethanedithiol). The reaction was subjected to 6 h of constant shaking (Labnet international). After completion of the reaction, the resin suspension was filtered, and the filtrate was collected, followed by the removal of TFA from the filtrate by nitrogen gas flow. The remaining filtrate was added to cold diethyl ether dropwise to ensure complete precipitation.

Finally, the precipitate was separated by centrifugation at 4 °C at 7000 rpm. All the peptides were purified by using a C-18 reverse-phase HPLC column and characterized using MALDI and HRMS mass spectrometry and stored in a –20 °C freezer for further use.

Purification of Peptides by Using HPLC and Characterization

The crude peptides (1 mg/mL) were dissolved in a solution of water and methanol (1:1; v/v) and loaded into a preparative RP-HPLC (Waters 1290 Infinity II Prep LC model using a Phenomenex TM column, LC-18, 250 \times 21.2 mm, 10 μ m), operating at 254 nm with a flow rate of 1 mL/min. The peptides were analyzed by using a mobile-phase solvent system (A) of 0.1% TFA in acetonitrile (CH_3CN) and (B) 0.1% TFA in water. Then, the system was run for 10 min as a linear gradient by using 10–70% of the mobile-phase B system. The desired fractions of the pure peptide were collected and concentrated. The peptides were dissolved in a minimum amount of ACN/water (1:1; v/v) solution and lyophilized. A fluffy white powder was collected, and the purity of the peptides was checked by analytical RP-HPLC (Waters 1290 Infinity II Prep LC model using a Phenomenex TM column, LC-18, 250 \times 21.2 mm, 10 μ m) operating at 254 nm with a flow rate of 1 mL/min. The mobile-phase solvent system was the same as the one used before, and the system was run for 20 min using a gradient of 10–60% of mobile-phase B. The purity of the peptides was in the range of 98–100%. Then, peptides were characterized by using HRMS.

Preparation of the $A\beta$ 42 Solution

We purchased synthetic Amyloid Beta Met—1–42 (1.0 mg) human from ALEXOTECH, with a purity of 95% characterized by HPLC and sodium dodecyl-sulfate polyacrylamide gel electrophoresis. The $A\beta$ 42 peptide (1 mg) was dissolved in 400 μ L of HFIP and stored at –20 °C to maintain the monomer state of the $A\beta$ 42 peptide. At the time of the experiment, the $A\beta$ 42 peptide solution in HFIP was taken out, HFIP was removed through gentle nitrogen gas flow, and a white solid residue was collected. The white solid $A\beta$ 42 peptide was dissolved in a minimum amount of a 1% NH_4OH solution. Then, a phosphate-buffered saline (PBS) (pH = 7.4) solution was used to make the required concentration of the $A\beta$ 42 peptide.

Preparation of $A\beta$ 42 Fibril Aggregates

The solution of the $A\beta$ 42 peptide (4 μ L) in HFIP was taken out and dried using a gentle flow of nitrogen gas. Then, the remaining solid $A\beta$ 42 peptide was dissolved in a 1% NH_4OH solution which was then diluted in 30 μ L of PBS solution (pH = 7.4) to 80 μ M. For the fibril aggregates, the $A\beta$ 42 solution was incubated at 37 °C for 72 h with gentle and constant shaking. The formation of $A\beta$ 42 fibril aggregates was confirmed by the ThT assay.

ThT Assay

For the confirmation of fibrils by the ThT assay, we used the incubated $A\beta$ 42 peptide solution in PBS (pH = 7.4). For the control experiment, the $A\beta$ 42 peptide (10 μ M in final conc.) monomer solution in PBS was taken and ThT solution (2 μ M in final conc.) was added to it; then, the fluorescence spectrum was recorded (λ_{ex} = 435 nm and λ_{em} = 445–800 nm). For the $A\beta$ 42 fibril aggregates, the incubated $A\beta$ 42 solution (10 μ M in final conc.) in PBS was taken, the ThT solution (2 μ M in final conc.) was added to it, and the fluorescence spectrum was recorded (λ_{ex} = 435 nm and λ_{em} = 445–800 nm).

$A\beta$ 42 Peptide Aggregation Inhibition

For $A\beta$ 42 peptide aggregation inhibition, we used a 5 μ M concentration of the $A\beta$ 42 peptide in the final volume and three different concentrations of the peptide (5, 10, 20, 40, 80, and 160 μ M) were used in the final volume. First, the $A\beta$ 42 peptide (5 μ M in final conc.) monomer solution in PBS was taken, and the peptide solution in PBS was added to it and incubated at 37 °C for 72 h with constant shaking. Then, the incubated solutions were taken out and the ThT solution (1 μ M in final volume) was added to it, followed by recording the fluorescence spectrum at λ_{ex} = 435 nm and λ_{em} = 445–800 nm. For time-dependent aggregation inhibition, the $A\beta$ 42 peptide

(5 μM in final conc.) monomer solution in PBS was taken and the peptide (10 μM in final volume) solution in PBS was added to it and incubated at 37 $^{\circ}\text{C}$ for 7 days continuously with constant shaking. At the time intervals of 24, 48, 72, 96, 120, 144, and 168 h, the incubated solution aliquots were taken out and ThT solution (1 μM in final volume) was added to it, followed by recording the fluorescence spectrum at $\lambda_{\text{ex}} = 435 \text{ nm}$ and $\lambda_{\text{em}} = 445\text{--}800 \text{ nm}$.

ITC Analysis

The ITC experiment was performed at a fixed temperature (298 K) in the PBS solution (0.1 mM) for the A β 42 (20 μM) and NT peptides. At every 5 min interval, 10 μL of the peptide was added by a computer control program with continuous stirring. For this ITC experiment, we performed 28 injections for each experiment. Every peak in the binding isotherm represents the interaction of the peptide with the A β 42 peptide. Finally, with the successive addition of the peptide, heat was released and analyzed. Then, the amount of heat released was plotted against the molar ratio of the peptide to the A β 42 peptide.

Dot Blot Assay

For the dot blot assay, the A β 42 (10 μM in final volume) solution was taken, and to this, various concentrations of the peptide (5, 10, and 20 μM in final volume) solution were added. Then, all the solutions were incubated at 37 $^{\circ}\text{C}$ for 72 h with gentle and constant shaking. After completion, 2 μL of the incubated solution was spotted on the nitrocellulose membrane and kept under air for 5 min or more until the spots had completely dried on the nitrocellulose membrane. For blocking of nonspecific sites, the nitrocellulose membrane was incubated in a solution of 5% bovine serum albumin in a TBS-T (Tris-buffered saline with 0.1% Tween 20 Detergent) buffer solution for 1 h at room temperature. Then, the nitrocellulose membranes were treated with primary antibody 6E10 (1:3000) to detect all forms of the A β peptide, A11 (1:1000) to detect the A β oligomers, and antibody OC (1:1000) to detect A β fibrillary aggregates, followed by incubating the membranes overnight at 4 $^{\circ}\text{C}$. After overnight incubation, the membranes were washed with TBS-T buffer three times for 3–5 min each. Then, horseradish peroxidase-conjugated antimouse secondary antibody (1:10,000) and antirabbit secondary antibody (1:10,000) were added to them and they were incubated for 2 h at room temperature followed by three washes with TBS-T buffer for 3–5 min each. Finally, an enhanced chemiluminescence reagent was added to the membrane and it was incubated, and readings of chemiluminescence were taken at several different lengths of exposure using ChemiDoc Azure Biosystem C400.

Molecular Docking

For the docking experiment, we took the A β 42 peptide (PDB ID: 1Z0Q) from the Protein Data Bank and the protein file was made by using Auto Dock Tools 1.5.6 software. Then, we drew the NT peptide structure using Avogadro software and optimized the NT peptide structure by using the CHARMM36 force field method. Then, we made the ligand files by using Auto Dock Tools 1.5.6 software. The optimized NT peptide assists as the input ligand, and the rigid protein A β 42 (PDB ID: 1Z0Q) was used as the macromolecule receptor. The grid box centered on the protein was defined with a dimension of 52 \times 26 \times 26 using a 1 \AA grid step, which is great enough to cover the whole A β 42 peptide and leave enough space for docking the ligand on the surface. Finally, we performed the molecular docking procedure using the AutoDock Vina (version 1.1.2) according to the Lamarckian genetic algorithm method. The binding modes were studied by using PyMol 2.5.

Cell Uptake and Cell Viability

For the cellular uptake of the NT peptides, PC-12 cells were plated in 35 mm glass-bottom confocal dishes. The cell was cultured for 24 h in a 5% CO₂ incubator at 37 $^{\circ}\text{C}$. After reaching 60–70% of the population, the cells were differentiated into neurons by treating the cells with 100 ng/mL NGF prepared in DMEM with reduced horse serum. A differentiated neuron morphology was observed (Figure S6) by immunocytochemistry experiments through microtubule staining

in PC12-derived neurons using corresponding primary and secondary antibodies following our previously standardized protocol.³⁵ Then, the differentiated PC-12 derived neurons were treated with 5(6)-carboxyfluorescein-attached NT peptides and incubated for another 6 h, then washed gently once with 1 \times PBS, and fixed for 45 min using 4% formaldehyde in an incubator. Again, after washing once with 1 \times PBS, finally, imaging was done using a fluorescence microscope (OLYMPUS IX83) using a 40 \times objective. Images were processed using Image J software. The cellular toxicity of our peptides was checked in differentiated PC-12-derived neurons using the MTT reduction method. For this experiment, PC-12 cells were seeded at a low density of 1 \times 10⁴ cells per well in a 96-well plate and incubated for 24 h at 37 $^{\circ}\text{C}$ under 5% CO₂ conditions. After 50–60% confluence, the cells were differentiated into neurons by treating the cells with 100 ng/mL NGF prepared in DMEM with reduced horse serum. Then, the differentiated PC-12-derived neurons were treated with three different concentrations of the peptide (5, 10, 20, 40, 80, and 160 μM) and incubated for 24 h at 37 $^{\circ}\text{C}$ under 5% CO₂ conditions. Then, to check the toxicity effect of the peptides in PC-12 neurons, 50 μL of the MTT solution (5 mg/mL) in PBS was added into each well and further incubated for 4 h at 37 $^{\circ}\text{C}$. Then, the medium was discarded and 50 μL of DMSO/methanol (1:1 v/v) was added to each well to dissolve the formazan. The absorbance was measured using a microplate reader (Thermo Scientific; Varioskan LUX) at 570 nm. Using these absorbance data, the percent viability of the cells was calculated following the method given below.

$$\text{Cell viability (\%)} = \frac{[\text{A570 (treated cells)} - \text{A570 (blank)}]}{[\text{A570 (control cells)} - \text{A570 (blank)}]} \times 100$$

Neuroprotection Effect of Peptides

For the neuroprotection effect of the peptides or restoring the cell viability in the presence of A β 42 mediated toxicity was performed in PC-12 derived neurons. For this, these PC-12 cells were seeded at a low density of 1 \times 10⁴ cells per well in a 96-well plate and incubated for 24 h at 37 $^{\circ}\text{C}$ under 5% CO₂ conditions. After 50–60% confluence, the cells were differentiated into neurons by treating the cells with 100 ng/mL NGF prepared in DMEM with reduced horse serum. Then, the cells were treated with A β 42 (5 μM) and individual peptides (5, 10, 20, 40, 80, and 160 μM) and incubated for 24 h at 37 $^{\circ}\text{C}$ under 5% CO₂ conditions. Then, to check the neuroprotection effect of the peptides in PC-12 neurons, 50 μL of MTT solution (5 mg/mL) in PBS was added into each well and further incubated for 4 h at 37 $^{\circ}\text{C}$. After 4 h, the media were discarded, and then formazan was dissolved with DMSO/MeOH (1:1 v/v). Finally, the absorption intensity of formazan was determined as a function of viable cells at 570 nm using a microplate reader (Thermo Scientific; Varioskan LUX). The absorbance data were used to calculate the percent viability of the cells by previously following the equation used in the MTT assay.

Apoptosis Assay

In a 96-well plate, PC-12 cells were seeded (1 \times 10⁴ cells per well) and incubated for 24 h at 37 $^{\circ}\text{C}$; after 50–60% confluence, the cells were treated with 100 ng/mL NGF for differentiation into neurons. Then, the differentiated neuronal cells were treated with A β 42 (10 μM) alone and A β 42 (10 μM) with NT peptides (10 μM) and then incubated for 24 h. After 24 h, neurons were washed with PBS buffer. Then, the neurons were stained with Calcein AM and PI. The fluorescence images were obtained using an Olympus fluorescence microscope. Apoptosis was analyzed and quantified using ImageJ software.

FTIR Spectroscopy Experiment

For the FTIR spectroscopy experiment, we used the A β 42 (20 μM) peptide monomer solution in PBS (pH = 7.4) and individual peptides (20 μM) were added and incubated at 37 $^{\circ}\text{C}$ for 1 week. For the control experiment, the A β 42 peptide (20 μM) was incubated alone. After incubation, solutions were centrifuged at 12,000 rpm for 10 min,

the supernatant solution was taken out, and the remaining small quantity of the precipitate was collected and freeze-dried. Then, the precipitate was dissolved in acetonitrile and subjected to FTIR spectroscopy (PerkinElmer Spectrum Version 10.5.3).

CD Spectroscopy

To check the β -sheet content by the CD experiment, we took the A β 42 (5 μ M) peptide monomer solution in PBS (pH = 7.4), and to these, individual peptides (5, 10, and 20 μ M) were added and incubated at 37 °C for 1 week with gentle and constant shaking. For the control experiment, the A β 42 (5 μ M) peptide was incubated alone. After completion of incubation, the solutions were inspected by CD spectroscopy using a JASCO (J-810) spectrometer.

Fluorescence Microscopy

For fluorescence microscopy imaging, we took 5 μ L of the solution from the A β 42 (10 μ M) alone and A β 42 (10 μ M) with NT peptides (10 μ M) incubated for 7 days. For the analysis, incubated solutions were taken at interval times of 24, 48, 72, 96, 120, 144, and 168 h; the incubated solution was taken out and spotted on a glass slide separately. Then, we added a 4 μ M solution of ThT or CR on the slide, and a cover slip was immediately placed over the sample. Images were captured using a fluorescence microscope (OLYMPUS IX83) using a 10 \times objective.

Serum Stability

For the stability of peptides in the physiological environment or serum condition, the peptides (150 μ M in final volume) were incubated with 50% human serum at 37 °C. For the analysis of peptides, at different time intervals (0, 6, 12, 24, 48, and 72 h), 100 μ L aliquots were taken out from the incubated solution and diluted with 100 μ L of acetonitrile for precipitating serum proteins; then, the solution was incubated at 4 °C for 30 min to stop the protease activity. After 30 min of incubation, samples were taken out and centrifuged at 10,000 rpm for 30 min at 4 °C. Then, the supernatant solution was collected. For the blank experiment, we used only the free serum solution without any compound. Finally, these supernatant solutions were analyzed by reverse-phase HPLC. The same procedure was used for all the time intervals.

BBB Crossing

In our laboratory, we used female pathogen-free C57BL/6J mice (8–10 weeks) for the BBB crossing experiment. All animal experiments were conducted following the laws and regulations of the regulatory authorities of our Institutional Animal Ethics Committee. For the BBB permeability test, we used 12 mice and divided them into 4 groups (3 mice/group). Peptide NT-02, NT-03, and NT-13 (100 μ L) (dosage of 5 mg/kg body weight of mice) solutions were injected intraperitoneally into the three different groups of mice separately (Table S7). For the control experiment, sucrose was dissolved in a normal saline solution and 100 μ L was injected into the last group of mice. After 6 h, mice were anesthetized with Avertin (IP) and sacrificed. Transcardial perfusion was performed to remove the blood from the body. Then, we removed the blood vessel and meninges, after which the brains were collected in PBS solutions. The brain cortical region was dissected and used for further analysis. Then, the cortex was homogenized in liquid nitrogen and extracted in acetonitrile. The acetonitrile suspension was centrifuged, the supernatant was collected, and then it was inspected using HRMS.

Data Analysis

Dot blots were analyzed by ImageJ software. For the measurement of spectroscopic data and histograms, we used Origin 8.5 pro software. Error bars represent mean \pm standard deviation (SD), $n = 3$. Statistical data were analyzed by the one-way ANOVA test by the multiple comparison test ($*p < 0.05$, $**p < 0.01$, $***p < 0.001$, $****p < 0.0001$, vs control or A β 42) using software GraphPad Prism (ISI, San Diego, CA).

ASSOCIATED CONTENT

Supporting Information

The Supporting Information is available free of charge at <https://pubs.acs.org/doi/10.1021/acsbiochemau.2c00067>.

Experimental details, figures, HRMS, and MALDI mass spectra (PDF)

AUTHOR INFORMATION

Corresponding Author

Surajit Ghosh – Department of Bioscience & Bioengineering, Indian Institute of Technology, Karwar, Rajasthan 342037, India; Organic and Medicinal Chemistry and Structural Biology and Bioinformatics Division, CSIR-Indian Institute of Chemical Biology, Kolkata, West Bengal 700 032, India; National Institute of Pharmaceutical Education and Research, Kolkata 700054, India; orcid.org/0000-0002-8203-8613; Phone: +91-291-280-1212; Email: sghosh@iitj.ac.in

Authors

Rathnam Malleesh – Department of Bioscience & Bioengineering, Indian Institute of Technology, Karwar, Rajasthan 342037, India; Organic and Medicinal Chemistry and Structural Biology and Bioinformatics Division, CSIR-Indian Institute of Chemical Biology, Kolkata, West Bengal 700 032, India; National Institute of Pharmaceutical Education and Research, Kolkata 700054, India; orcid.org/0000-0001-5609-047X

Juhee Khan – Department of Bioscience & Bioengineering, Indian Institute of Technology, Karwar, Rajasthan 342037, India; Organic and Medicinal Chemistry and Structural Biology and Bioinformatics Division, CSIR-Indian Institute of Chemical Biology, Kolkata, West Bengal 700 032, India; orcid.org/0000-0002-9955-6505

Prabir Kumar Gharai – Department of Bioscience & Bioengineering, Indian Institute of Technology, Karwar, Rajasthan 342037, India; Organic and Medicinal Chemistry and Structural Biology and Bioinformatics Division, CSIR-Indian Institute of Chemical Biology, Kolkata, West Bengal 700 032, India; orcid.org/0000-0002-1383-9521

Varsha Gupta – Department of Bioscience & Bioengineering, Indian Institute of Technology, Karwar, Rajasthan 342037, India; Organic and Medicinal Chemistry and Structural Biology and Bioinformatics Division, CSIR-Indian Institute of Chemical Biology, Kolkata, West Bengal 700 032, India

Rajsekhar Roy – Department of Bioscience & Bioengineering, Indian Institute of Technology, Karwar, Rajasthan 342037, India

Complete contact information is available at: <https://pubs.acs.org/10.1021/acsbiochemau.2c00067>

Author Contributions

R.M. performed the synthesis, purification, and characterization of all peptides and all the in vitro assays, dot blot experiments, and molecular docking studies. J.K. performed the BBB experiment and cell-based assays. V.G. performed the cell uptake experiment. P.K.G. and R.R. helped with the conduction of various experiments and helped to analyze the data and various experiments. S.G. conceived the idea, supervised the project, and wrote the manuscript. CREdiT:

Rathnam Mallesh conceptualization (supporting), data curation (equal), formal analysis (equal), investigation (equal), methodology (equal), visualization (equal), writing-original draft (equal), writing-review & editing (equal); **Juheh Khan** data curation (supporting), formal analysis (supporting), investigation (supporting), methodology (supporting), writing-original draft (supporting), writing-review & editing (supporting); **Prabir Kumar Gharai** data curation (supporting), methodology (supporting), writing-original draft (supporting); **Varsha Gupta** data curation (supporting), investigation (supporting); **Rajsekhar Roy** data curation (supporting), formal analysis (supporting), investigation (supporting), methodology (supporting), writing-review & editing (supporting); **Surajit Ghosh** conceptualization (lead), formal analysis (lead), funding acquisition (lead), investigation (lead), methodology (lead), project administration (lead), resources (lead), supervision (lead), validation (lead), writing-original draft (lead), writing-review & editing (lead).

Funding

This work was supported by the DST-SERB, India (CRG/2019/000670).

Notes

The authors declare no competing financial interest.

ACKNOWLEDGMENTS

R.M. thanks the NIPER for providing his fellowship; J.K. and V.G. thank DST-INSPIRE for their fellowship; P.K.G. thanks the CSIR for his fellowship; R.R. thanks IIT Jodhpur for providing his fellowship. S.G. kindly acknowledges the DST-SERB, India (CRG/2019/000670), for financial support. We thank CSIR-IICB Kolkata and IIT Jodhpur for providing infrastructure.

ABBREVIATIONS

AD	Alzheimer's disease
APP	amyloid beta precursor protein
A β	amyloid beta
PS1	presenilin 1
BBB	blood-brain barrier
ThT	thioflavin-T
PDB	Protein Data Bank
SD	standard deviation
PBS	phosphate-buffered saline
DMEM	Dulbecco's modified Eagle medium
MTT	3-(4,5-dimethylthiazol-2-yl)-2,5-diphenyl tetrazolium bromide
DCM	dichloromethane
ACN	acetonitrile
THF	tetrahydrofuran
DMF	N,N-dimethylformamide
DMSO	dimethyl sulfoxide
NH ₄ OH	ammonium hydroxide
HFIP	1,1,1,3,3,3-hexafluoro-2-propanol
HRMS	high-resolution mass spectroscopy

REFERENCES

- (1) Wong, C. W.; Quaranta, V.; Glenner, G. G. Neuritic Plaques and Cerebrovascular Amyloid in Alzheimer Disease Are Antigenically Related. *Proc. Natl. Acad. Sci.* **1985**, *82*, 8729–8732.
- (2) Glenner, G. G.; Wong, C. W. Alzheimer's Disease: Initial Report of the Purification and Characterization of a Novel Cerebrovascular

Amyloid Protein. *Biochem. Biophys. Res. Commun.* **1984**, *120*, 885–890.

(3) Roher, A. E.; Lowenson, J. D.; Clarke, S.; Woods, A. S.; Cotter, R. J.; Gowing, E.; Ball, M. J. Beta-Amyloid-(1-42) Is a Major Component of Cerebrovascular Amyloid Deposits: Implications for the Pathology of Alzheimer Disease. *Proc. Natl. Acad. Sci.* **1993**, *90*, 10836–10840.

(4) Selkoe, D. J. Amyloid β -Protein and the Genetics of Alzheimer's Disease. *J. Biol. Chem.* **1996**, *271*, 18295–18298.

(5) Terzi, E.; Hölzemann, G.; Seelig, J. Self-Association of β -Amyloid Peptide (1–40) in Solution and Binding to Lipid Membranes. *J. Mol. Biol.* **1995**, *252*, 633–642.

(6) Kang, J.; Lemaire, H.-G.; Unterbeck, A.; Salbaum, J. M.; Masters, C. L.; Grzeschik, K.-H.; Multhaup, G.; Beyreuther, K.; Müller-Hill, B. The Precursor of Alzheimer's Disease Amyloid A4 Protein Resembles a Cell-Surface Receptor. *Nature* **1987**, *325*, 733–736.

(7) Tamaoka, A.; Odaka, A.; Ishibashi, Y.; Usami, M.; Sahara, N.; Suzuki, N.; Nukina, N.; Mizusawa, H.; Shoji, S.; Kanazawa, I. APP717 Missense Mutation Affects the Ratio of Amyloid Beta Protein Species (A β 1-42/43 and a β 1-40) in Familial Alzheimer's Disease Brain. *J. Biol. Chem.* **1994**, *269*, 32721–32724.

(8) Lomakin, A.; Chung, D. S.; Benedek, G. B.; Kirschner, D. A.; Teplow, D. B. On the Nucleation and Growth of Amyloid Beta-Protein Fibrils: Detection of Nuclei and Quantitation of Rate Constants. *Proc. Natl. Acad. Sci.* **1996**, *93*, 1125–1129.

(9) Roychaudhuri, R.; Yang, M.; Hoshi, M. M.; Teplow, D. B. Amyloid β -Protein Assembly and Alzheimer Disease. *J. Biol. Chem.* **2009**, *284*, 4749–4753.

(10) Goldsbury, C. S.; Wirtz, S.; Müller, S. A.; Sunderji, S.; Wicki, P.; Aebi, U.; Frey, P. Studies on the In Vitro Assembly of A β 1–40: Implications for the Search for A β Fibril Formation Inhibitors. *J. Struct. Biol.* **2000**, *130*, 217–231.

(11) Pike, C. J.; Walencewicz-Wasserman, A. J.; Kosmoski, J.; Cribbs, D. H.; Glabe, C. G.; Cotman, C. W. Structure-Activity Analyses of β -Amyloid Peptides: Contributions of the B25–35 Region to Aggregation and Neurotoxicity. *J. Neurochem.* **1995**, *64*, 253–265.

(12) Soto, C.; Castaño, E. M.; Frangione, B.; Inestrosa, N. C. The α -Helical to β -Strand Transition in the Amino-Terminal Fragment of the Amyloid β -Peptide Modulates Amyloid Formation. *J. Biol. Chem.* **1995**, *270*, 3063–3067.

(13) Hilbich, C.; Kisters-Woike, B.; Reed, J.; Masters, C. L.; Beyreuther, K. Substitutions of Hydrophobic Amino Acids Reduce the Amyloidogenicity of Alzheimer's Disease BA4 Peptides. *J. Mol. Biol.* **1992**, *228*, 460–473.

(14) Tjernberg, L. O.; Näslund, J.; Lindqvist, F.; Johansson, J.; Karlström, A. R.; Thyberg, J.; Terenius, L.; Nordstedt, C. Arrest of β -Amyloid Fibril Formation by a Pentapeptide Ligand (*). *J. Biol. Chem.* **1996**, *271*, 8545–8548.

(15) Tjernberg, L. O.; Lilliehöök, C.; Callaway, D. J.; Näslund, J.; Hahne, S.; Thyberg, J.; Terenius, L.; Nordstedt, C. Controlling Amyloid Beta-Peptide Fibril Formation with Protease-Stable Ligands. *J. Biol. Chem.* **1997**, *272*, 12601–12605.

(16) Lyu, P. C.; Sherman, J. C.; Chen, A.; Kallenbach, N. R. Alpha-Helix Stabilization by Natural and Unnatural Amino Acids with Alkyl Side Chains. *Proc. Natl. Acad. Sci. U.S.A.* **1991**, *88*, 5317–5320.

(17) Li, S. C.; Goto, N. K.; Williams, K. A.; Deber, C. M. Alpha-Helical, but Not Beta-Sheet, Propensity of Proline Is Determined by Peptide Environment. *Proc. Natl. Acad. Sci. U.S.A.* **1996**, *93*, 6676–6681.

(18) Shearman, M. S.; Ragan, C. I.; Iversen, L. L. Inhibition of PC12 Cell Redox Activity Is a Specific, Early Indicator of the Mechanism of Beta-Amyloid-Mediated Cell Death. *Proc. Natl. Acad. Sci.* **1994**, *91*, 1470–1474.

(19) Liu, Y.; Peterson, D. A.; Kimura, H.; Schubert, D. Mechanism of Cellular 3-(4,5-Dimethylthiazol-2-Yl)-2,5-Diphenyltetrazolium Bromide (MTT) Reduction. *J. Neurochem.* **1997**, *69*, 581–593.

- (20) Mosmann, T. Rapid Colorimetric Assay for Cellular Growth and Survival: Application to Proliferation and Cytotoxicity Assays. *J. Immunol. Methods* **1983**, *65*, 55–63.
- (21) Levine, H., III Thioflavine T Interaction with Synthetic Alzheimer's Disease β -Amyloid Peptides: Detection of Amyloid Aggregation in Solution. *Protein Sci.* **1993**, *2*, 404–410.
- (22) Chou, P. Y.; Fasman, G. D. Empirical Predictions of Protein Conformation. *Annu. Rev. Biochem.* **1978**, *47*, 251–276.
- (23) Garnier, J.; Osguthorpe, D. J.; Robson, B. Analysis of the Accuracy and Implications of Simple Methods for Predicting the Secondary Structure of Globular Proteins. *J. Mol. Biol.* **1978**, *120*, 97–120.
- (24) Soto, C.; Brañes, M. C.; Alvarez, J.; Inestrosa, N. C. Structural Determinants of the Alzheimer's Amyloid β -Peptide. *J. Neurochem.* **1994**, *63*, 1191–1198.
- (25) Zagorski, M. G.; Barrow, C. J. NMR Studies of Amyloid β -Peptides: Proton Assignments, Secondary Structure, and Mechanism of an α -Helix \rightarrow β -Sheet Conversion for a Homologous, 28-Residue, N-Terminal Fragment. *Biochemistry* **1992**, *31*, 5621–5631.
- (26) Barrow, C. J.; Zagorski, M. G. Solution Structures of β Peptide and Its Constituent Fragments: Relation to Amyloid Deposition. *Science* **1991**, *253*, 179–182.
- (27) Hilbich, C.; Kisters-Woike, B.; Reed, J.; Masters, C. L.; Beyreuther, K. Aggregation and Secondary Structure of Synthetic Amyloid BA4 Peptides of Alzheimer's Disease. *J. Mol. Biol.* **1991**, *218*, 149–163.
- (28) Tomaselli, S.; Esposito, V.; Vangone, P.; van Nuland, N. A. J.; Bonvin, A. M. J. J.; Guerrini, R.; Tancredi, T.; Temussi, P. A.; Picone, D. The α -to- β Conformational Transition of Alzheimer's $A\beta$ -(1–42) Peptide in Aqueous Media Is Reversible: A Step by Step Conformational Analysis Suggests the Location of β Conformation Seeding. *ChemBioChem* **2006**, *7*, 257–267.
- (29) Surewicz, W. K.; Mantsch, H. H. New Insight into Protein Secondary Structure from Resolution-Enhanced Infrared Spectra. *Biochim. Biophys. Acta, Protein Struct. Mol. Enzymol.* **1988**, *952*, 115–130.
- (30) Byler, D. M.; Susi, H. Examination of the Secondary Structure of Proteins by Deconvolved FTIR Spectra. *Biopolymers* **1986**, *25*, 469–487.
- (31) Adler, A. J.; Greenfield, N. J.; Fasman, G. D. [27] Circular Dichroism and Optical Rotatory Dispersion of Proteins and Polypeptides. *Methods Enzymol.* **1973**, *27*, 675–735.
- (32) Pradhan, K.; Das, G.; Mondal, P.; Khan, J.; Barman, S.; Ghosh, S. Genesis of Neuroprotective Peptoid from $A\beta$ 30–34 Inhibits $A\beta$ Aggregation and AChE Activity. *ACS Chem. Neurosci.* **2018**, *9*, 2929–2940.
- (33) Hong, S. Y.; Oh, J. E.; Lee, K. H. Effect of D-Amino Acid Substitution on the Stability, the Secondary Structure, and the Activity of Membrane-Active Peptide. *Biochem. Pharmacol.* **1999**, *58*, 1775–1780.
- (34) Mallesh, R.; Khan, J.; Pradhan, K.; Roy, R.; Jana, N. R.; Jaisankar, P.; Ghosh, S. Design and Development of Benzothiazole-Based Fluorescent Probes for Selective Detection of $A\beta$ Aggregates in Alzheimer's Disease. *ACS Chem. Neurosci.* **2022**, *13*, 2503–2516.
- (35) Adak, A.; Das, G.; Barman, S.; Mohapatra, S.; Bhunia, D.; Jana, B.; Ghosh, S. Biodegradable Neuro-Compatible Peptide Hydrogel Promotes Neurite Outgrowth, Shows Significant Neuroprotection, and Delivers Anti-Alzheimer Drug. *ACS Appl. Mater. Interfaces* **2017**, *9*, 5067–5076.